Sustainable Materials and Technologies 33 (2022) e00497

Contents lists available at ScienceDirect

Sustainable Materials and Technologies

journal homepage: www.elsevier.com/locate/susmat

Heterofunctionalized polyphenolic dendrimers decorated with caffeic acid: Synthesis, characterization and antioxidant activity

Marika Grodzicka [a,b,1], Cornelia E. Pena-Gonzalez [c,1], Paula Ortega [c,d], Sylwia Michlewska [e,*], Rebeca Lozano [c], Maria Bryszewska [a], Francisco Javier de la Mata [c,d], Maksim Ionov [a]

[a] Department of General Biophysics, Faculty of Biology & Environmental Protection, University of Lodz, Pomorska 141/143, Lodz 90–236, Poland
[b] BioMedChem Doctoral School of the UL and Lodz Institutes of the Polish Academy of Science, Banacha 12/16, 0-237 Lodz, Poland
[c] Universidad de Alcalá, Department of Organic and Inorganic Chemistry, and Research Institute in Chemistry "Andrés M. del Río" (IQAR), Spain and Instituto Ramon y Cajal de Investigacion Sanitaria, IRYCIS, Colmenar Viejo Road, Km 9, 100, 28034 Madrid, Spain
[d] Networking Research Center on Bioengineering, Biomaterials and Nanomedicine (CIBER-BBN), Spain
[e] Laboratory of Microscopic Imaging & Specialized Biological Techniques, Faculty of Biology & Environmental Protection, University of Lodz, Banacha12/16, Lodz 90–237, Poland

ARTICLE INFO

Keywords:
Polyphenolic dendrimers
Synthesis
Caffeic acid
Antioxidant activity
Toxicity

ABSTRACT

Dendrimers, branched polymer structures, have been widely studied as efficient drug carriers. Scientists are trying to find new dendrimer-based formulations with the properties needed for biomedical applications such as improved bioavailability, low toxicity and high transfection profiles. The unique drug delivery properties of carbosilane dendrimers have already been demonstrated. Their efficacy has been further improved by conjugation with polyphenols, plant secondary metabolites with a wide range of biological activities, including antioxidant effects that are beneficial for human health. The present study focuses on synthesis and characterization of two new types of carbosilane dendritic systems, one family presents one or two caffeic acid units and ammonium groups on the surface to make them water soluble. The other family has, in addition to the two mentioned functionalities, one or two polyethylene glycol (PEG) chains in the structure to increase the biocompatibility of the system. Carbosilane dendrimers with caffeic acid have low toxicity and protect erythrocytes against oxidative hemolysis. These dendrimers also decrease AAPH-induced ROS production in human fibroblasts.

Various techniques demonstrating such antioxidant activities have been applied in the current research. The best antioxidant properties were shown for the dendrimer with two PEG-caffeic acid moieties. Further aspects of the biochemical characterization of the dendrimers are also considered and discussed.

1. Introduction

During the early 1980s, super-branched monodispersive nanoparticles named dendrimers were first synthesized by Tomalia's team [1,2]. Dendrimers are spherical, with a densely packed surface and free internal spaces. Owing to their unique architecture they are considered excellent transporters of drugs and genes [3]. They could be used to make cancer or neurodegenerative disease therapies more efficient. They are well defined and relatively easy to synthesize [4–10]. Dendrimers such as PAMAM, PPI, (see Table 1 "Abbreviations"), and carbosilane have been repeatedly described and their physicochemical and biological properties have been reported. Conjugation of drugs with dendrimers improves their solubility and bioavailability. Slow release of a drug from a drug/dendrimer complex sustains its circulation in the bloodstream and reduces the side effects of chemotherapeutics. Cationic dendrimers can form stable complexes with nucleic acids and have been suggested as promising carriers for genes for use in gene therapy. Moreover, nucleic acids complexed with dendrimers can interact with negatively-charged cell membranes [8,11–14]. On the other hand, positively charged dendrimers can be cytotoxic [8,15,16]. One way to decrease such toxicity is to conjugate them with polyethylene glycol (PEG) [17–20]. PEGylation can stabilize their interactions with nucleic acids and reduce interactions with serum proteins [6,20]. PEG also increases the solubility of dendrimers in water and limits their uptake by

* Corresponding author.
E-mail address: sylwia.michlewska@biol.uni.lodz.pl (S. Michlewska).
[1] These authors contributed equally to the work

https://doi.org/10.1016/j.susmat.2022.e00497
Received 20 April 2022; Received in revised form 26 August 2022; Accepted 16 September 2022
Available online 21 September 2022
2214-9937/

Table 1
Abbreviations.

A549	Cancer human alveolar basal epithelial cells
AAPH	2,2′-azobis-2-methyl-propanimidamide, dihydrochloride, Cayman, USA
BJ	Normal human fibroblasts
BODIPY581/591	(4,4-difluoro-5-(4-phenyl-1,3-butadienyl)-4-bora-3a,4a-diaza-s-indacene-3-un-decanoic acid; invitrogen, Thermo Fisher Scientific, USA
CD_3OD	Deuterated methanol
$CDCl_3$	Deuterated chloroform
DCF	2′,7′-dichlorofluorescein
DLS	Dynamic light-scattering
DMEM	Dulbecco's Modified Eagle Medium
DMF	Dimethylfuran
DMPA	2,2-dimethoxy-2-phenylaceto-phenone
DMSO	Dimethyl Sulfoxide, Avantor, Gliwice, Poland
DPPH	2,2′-diphenyl-1-picrylhydrazyl; Sigma Aldrich,
EDCI-HCl	1-Ethyl-3-(3-dimethylaminopropyl)carbodiimide hydrochloride
FBS	Fetal Bovine Serum
FRAP	Ferric Reducing Antioxidant Power
H_2DCF-DA	2′,7′-dichlorofluorescindiacetate; Thermo Fisher, Waltham, MA, USA
HOBt	1-Hydroxybenzotriazole hydrate
MTT	3-(4,5-Dimethyl-2-thiazolyl)-2,5-diphenyl-2H-tetrazolium bromide, Methylthiazolyldiphenyl-tetrazolium bromide; Sigma Aldrich, USA
NMR	Nuclear magnetic resonance
PAMAM	Poly(amidoamine)
PB	Na-phosphate buffer
PBS	Phosphate Buffered Saline
PDI	Polydispersity index
PEG	Polyethylene glycol
PPI	Poly(propylene imine)
ROS	Reactive oxygen species
RPMI 1640	Roswell Park Memorial Institute
TEAC	Trolox Equivalent Antioxidant Capacity
TEM	Transmission electron microscopy
TPTZ	2,4,6-tripyridyl-striazine

reticuloendothelial systems, prolonging their circulation time and increasing haemocompatibility [20,21].

Scientists continue to improve the properties of dendrimers, for example, by attaching anticancer metals such as gold, ruthenium, or copper to their surfaces [7,22–26]. Such metallodendrimers have been intensively studied for anticancer therapy. Other strategies include anchoring active biomolecules e.g. polyphenols such as caffeic, ferulic, and gallic acids in the nanoparticle structure. These modifications can increase the bioavailability of the polyphenols and confer antioxidative, antibacterial and other biological activities on the dendrimers [27,28]. This can be crucial in some cases since oxidative stress contributes to the development of such conditions as Alzheimer's and Parkinson's diseases, diabetes, rheumatoid arthritis, cardiovascular diseases, and cancers [29,30]. Antioxidants are undoubtedly beneficial for human health and protect cells against injuries caused by oxidative stress [31].

The polyphenol caffeic acid, present at high levels in coffee, has good antioxidant properties [32]. Numerous studies have indicated that coffee benefits people with diabetes [33], obesity [34] and cognitive deficits [35], suggesting that it contains physiologically active substances and could have anticancer effects. Coffee is reportedly beneficial in treating gastric [36], colorectal [37] and oral [38] cancers, and melanoma [39,40], possibly because it contains polyphenols and especially caffeic acid [41]. Apart from its antioxidant and anticancer properties, caffeic acid also has anticoagulant, antihypertensive, antifibrotic, and antiviral activities [42,43].

In order to combine these medical properties of caffeic acid with the drug delivery properties of dendrimers, a new class of polyphenolic dendrimers has been synthesized [44]. The present study investigates these cationic dendrimers, which comprise a carbosilane core functionalized with caffeic acid moieties. The manuscript focuses mainly on analyzing their antioxidant and antiradical properties. Their biophysical characterization, haemotoxicity and cytotoxicity are also considered. The scheme of the research is outlined in Fig. 1.

2. Material and methods

2.1. Synthesis and chemical characterization

All reactions took place under an inert atmosphere and the solvents used were bought in dry conditions. NMR spectra were recorded in a Varian 500 Hz spectrometer using $CDCl_3$ and CD_3OD as solvents. Chemical shifts (δ) are given in ppm. A LECO CHNS-932 instrument was used for all elemental analyses. The reagents HS-PEG-NH_2·HCl, 2,2-dimethoxy-2-phenylaceto-phenone (DMPA), HS-$(CH_2)_2NH_3Cl$, HS-$(CH_2)_2N(CH_3)_2HCl$, N-(3-Dimethylaminopropyl)-N′-ethylcarbodiimide hydrochloride (EDCI·HCl), 1-Hydroxybenzotriazole hydrate (HOBt), $NaBH_4$, Amberlite IRA-Cl and caffeic acid were purchased from sigma addrich.

The supporting material details the synthesis and characterization of dendrimers **II**, **III**, and **1**–**10**. We describe the polyphenolic derivatives here.

2.1.1. Synthesis of G_2-[(S-$(CH_2)_2$NH(CO)CH=CHCH$_2$Ph(OH)$_2$)(S-N$(CH_3)_2)_7$] (11)

First, caffeic acid (96.8 mg, 0.537 mM) was activated with EDCI-HCl (102.73 mg, 0.537 mM) and HOBt (75.3 mg, 0.537 mM) using dry Dimethylformamide (DMF) as solvent. The mixture was stirred for 1 h at room temperature, then a DMF solution of the dendrimer G_2-[(S-NH_2)(S-N$(CH_3)_2)_7$] (**7**) (375.8 mg, 0.268 mM) was added dropwise at 0 °C with stirring. The mixture was maintained in this condition for 5 min, incubated at 60 °C overnight, and then treated with Na_2CO_3 (243.6 mg, 2.25 mM) for 3 h, filtered, and purified by size exclusion chromatography in DMF. The solvent was eliminated under vacuum, leaving compound **11** as an orange oil (267.81 mg, 59.3%).

^{1}H NMR (CD_3OD): δ (ppm) 0.06 (s, 12H, SiCH_3), 0.64 (m, 8H, SiCH_2CH$_2$CH$_2$Si), 0.70 (m, 8H, SiCH$_2$CH$_2$$CH_2$Si), 0.93 (m, 16H, Si$CH_2CH_2$S), 1.40 (m, 8H, SiCH$_2$$CH_2CH_2$Si), 2.27 (s, 42H, N$CH_3$), 2.55 (m, 14H, SCH$_2$$CH_2NCH_3$), 2.57–2.67 (m, overlapping of signals, 28H, SiCH$_2$$CH_2$S and S$CH_2CH_2NCH_3$), 2.71 (m, 2H, S$CH_2CH_2$NH), 3.47 (m, 2H, SCH$_2$$CH_2$NH), 6.36 (d, 1H, $^3J_{(H-H)}$ = 15.7 Hz, PhC*H*=CH(*CO*)NH), 6.76 (d, 1H, $^3J_{(H-H)}$ = 8.1 Hz, 1H$_{Ar}$, *meta-CH=CH*), 6.90 (d, 1H, $^3J_{(H-H)}$ = 8.2 Hz, 1H$_{Ar}$, *orto-CH=CH*), 7.01 (s, 1H, 1H$_{Ar}$, *orto-CH=CH, orto-OH*), 7.41 (d, 1H, $^3J_{(H-H)}$ = 15.7 Hz, PhCH=C*H*(*CO*)NH). **^{13}C {^{1}H}-NMR (CD_3OD):** δ (ppm) -6.2 SiCH$_3$), 14.3 (SiCH$_2$CH$_2$S), 17.2 (SiCH$_2$CH$_2$CH$_2$Si), 18.5 (SiCH$_2$CH$_2$CH$_2$Si), 27.2 (SiCH$_2$CH$_2$S), 28.4 (SCH$_2$CH$_2$NCH$_3$), 30.7 (SCH$_2$CH$_2$NH), 39.2 (SCH$_2$CH$_2$NH), 44.0 (NCH$_3$), 58.9 (SiCH$_2$CH$_2$NCH$_3$), 113.7 (CAr, *orto-OH, orto-CH=CH*), 115.1 (CAr, *meta-CH=CH*), 116.9 (PhCH=CH(*CO*)NH), 120.8, (CAr, *orto-CH=CH*), 141.0 (PhCH=*CH*(*CO*)NH), not observed (Cipso), not observed (NHC=O). **Elemental Analysis (%):** Calc for $C_{71}H_{150}N_8O_3S_8Si_5$ (1560.94 g/mol). C, 54.63; H, 9.69; N, 7.18. Exp.: C, 54.51; H, 8.727; N, 7.328;

2.1.2. Synthesis of G_2-[(S-$(CH_2)_2$NH(CO)CH=CHCH$_2$Ph(OH)$_2$)$_2$(S-N$(CH_3)_2)_6$] (12)

Dendrimer **12** was prepared by the same method as **11** using the following reagents: caffeic acid (104.8 mg, 0.546 mM), EDCI·HCl (105.5 mg, 0.545 mM), HOBt (72.6 mg, 0.545 mM), G_2-[(S-NH_2)(S-N$(CH_3)_2)_7$] (**8**) (187.0 mg, 0.136 mM) and Na_2CO_3 (86.74 mg, 0.818 mM). Compound **12** was obtained as an orange oil (138.7 mg, 68%).

^{1}H NMR (CD_3OD): δ (ppm) 0.06 (s, 12H, SiCH_3), 0.66 (m, 8H, SiCH_2CH$_2$CH$_2$Si), 0.72 (m, 8H, SiCH$_2$CH$_2$$CH_2$Si), 0.95 (m, 16H, Si$CH_2CH_2$S), 1.42 (m, 8H, SiCH$_2$$CH_2CH_2$Si), 2.28 (s, 36H, N$CH_3$), 2.55 (m, 12H, S$CH_2CH_2NCH_3$), 2.58–2.69 (m, overlapping of signals, 32H, SiCH$_2$$CH_2S, SCH_2$$CH_2NCH_3$ and SCH_2CH$_2$NH), 3.47 (m, 4H, OCH$_2$$CH_2$NH), 6.41 (d, 2H, $^3J_{(H-H)}$ = 15.7 Hz, PhC*H*=CH(*CO*)NH), 6.76 (d, 2H, $^3J_{(H-H)}$ = 8.1 Hz, H$_{Ar}$, *meta-CH=CH*), 6.90 (d, 2H, $^3J_{(H-H)}$ = 8.2

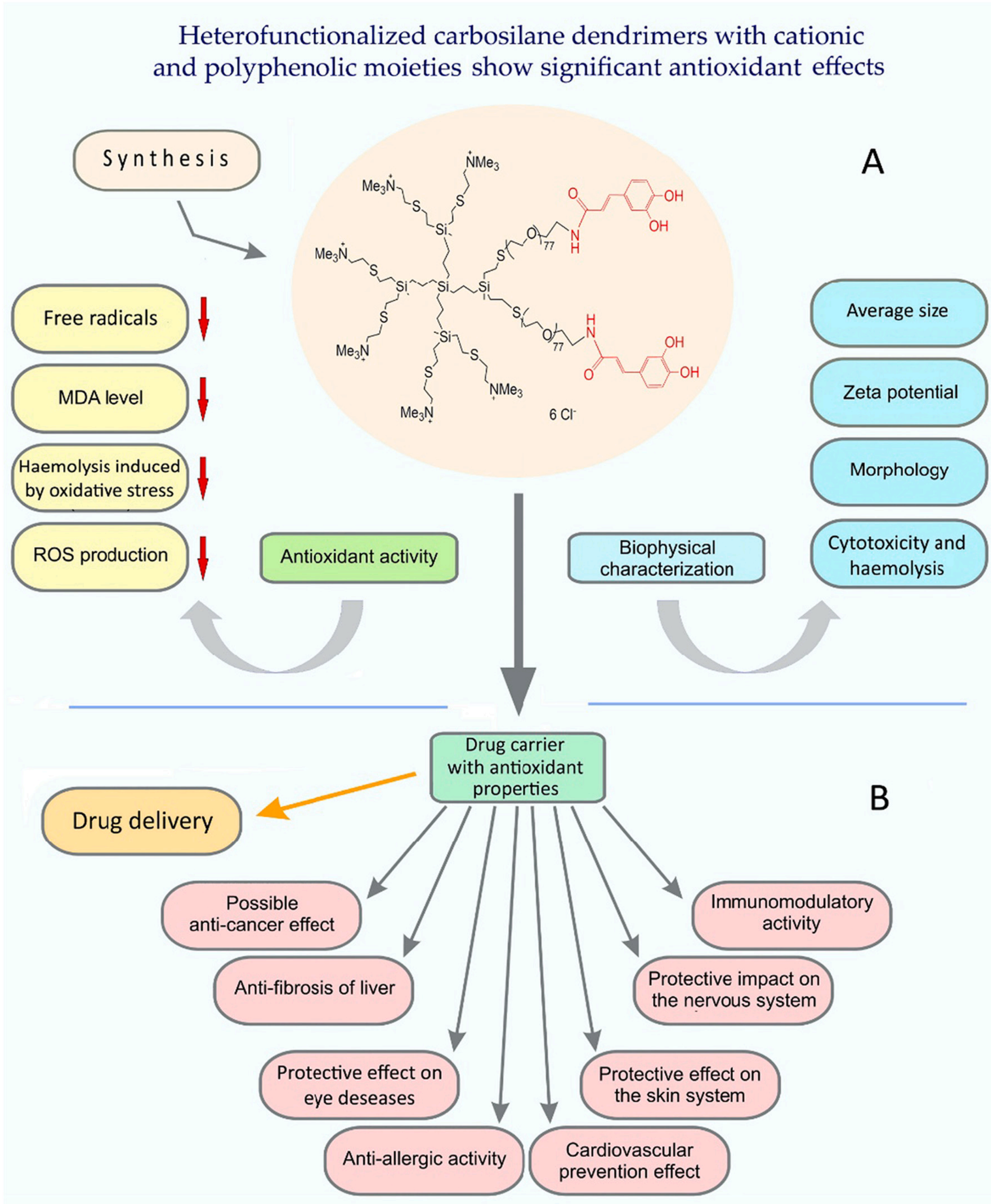

Fig. 1. (A) Schematic drawing of the research. Antioxidant effects (left) and biophysical properties (right) of polyphenolic dendrimers considered in this study. (B) Possible (expected) protective effects against various injuries to body systems resulting from antioxidant activity.

Hz, H_{Ar}, *orto-CH*=*CH*), 7.01 (s, 2H, H_{Ar}, *orto-CH*=*CH, orto-OH*), 7.41 (d, 2H, $^3J_{(H-H)}$ = 15.7 Hz, PhCH=C*H*(*CO*)NH). **^{13}C {^{1}H}-NMR (CD_3OD):** δ (ppm) -6.1 Si*C*H_3), 14.3 (Si*C*H_2CH_2S), 17.1 (SiCH_2CH_2*C*H_2Si), 18.0 (SiCH_2*C*H_2CH_2Si), 18.3 (Si*C*$H_2CH_2CH_2$Si), 27.2 (SiCH_2*C*H_2S), 28.4 (S*C*$H_2CH_2NCH_3$), 30.7 (S*C*H_2CH_2NH), 39.2 (SCH_2*C*H_2NH), 44.0 (N*C*H_3*)*, 58.9 (SCH_2*C*H_2NCH_3), 113.7 (CAr, *orto-OH, orto-CH*=*CH*), 115.1 (CAr, *meta-CH*=*CH*), 116.9 (Ph*C*H=CH(*CO*)NH*)*, 120.8, (CAr, *orto-CH*=*CH*), 126.8 (Cipso, *meta-OH, para-OH*), 141.0 (PhCH=*C*H(*CO*) NH), not observed (NH*C*=O). **Elemental Analysis (%):** Calc for $C_{78}H_{152}N_8O_6S_8Si_5$ (1695.03 g/mol). C, 55.27; H, 9.04; N, 6.61. Exp.: C, 54.58; H, 8.85; N, 6.542.

2.1.3. Synthesis of G_2-[(S-PEG-NH(CO)CH=CHCH$_2$Ph(OH)$_2$)(S-N (CH$_3$)$_2$)$_7$] (13)

Dendrimer **13** was prepared by the same method as **11** using the following reagents: caffeic acid (19.09 mg, 0.106 mM), EDCI·HCl (20.3 mg, 0.106 mM), HOBt (14.11 mg, 0.106 mM), G_2-[(S-PEG-NH_2)(S-N (CH_3)$_2$)$_7$] (**9**) (253.6 mg, 0.053 mM), Na_2CO_3 (47.19 mg, 0.445 mM). Compound **13** was obtained an orange oil (123.2 mg, 45%).

^{1}H NMR (CD_3OD):δ (ppm) 0.08 (s, 12H, Si*C*H_3), 0.65 (m, 8H, Si*C*$H_2CH_2CH_2$Si), 0.71 (m, 8H, SiCH_2CH_2*C*H_2Si), 0.96 (m, 16H, Si*C*H_2CH_2S), 1.42 (m, 8H, SiCH_2*C*H_2CH_2Si), 2.29 (s, 42H, N*C*H_3), 2.55 (m, 14H, SCH_2*C*H_2NCH_3), 2.59–2.75 (m, overlapping of signals, 32H, SiCH_2*C*H_2S, S*C*$H_2CH_2NCH_3$ and S-*C*H_2CH_2O), 3.48 (m, 2H,

OCH_2CH_2NH), 3.58–3.69 (m, 308H, OCH_2), 6.42 (d, 1H, $^3J_{(H—H)}$ = 15.7 Hz, PhCH=CH(CO)NH), 6.77 (d, 1H, $^3J_{(H—H)}$ = 8.2 Hz, $1H_{Ar}$, *meta-CH=CH*), 6.92 (dd, 1H, $^3J_{(H—H)}$ = 8.2 Hz, $^5J_{(H—H)}$ = 2.1 Hz, $1H_{Ar}$, *ortho-CH=CH*), 7.02 (d, 1H, $^5J_{(H—H)}$ = 2.1 Hz, $2H_{Ar}$, *ortho-CH=CH, ortho-OH*), 7.40 (d, 1H, $^3J_{(H—H)}$ = 15.7 Hz, PhCH=CH(CO)NH). **^{13}C {^{1}H}-NMR (CD_3OD):** δ (ppm) -6.4 $SiCH_3$), 14.3 ($SiCH_2CH_2S$), 16.9 ($SiCH_2CH_2CH_2Si$), 18.0 ($SiCH_2CH_2CH_2Si$), 27.1 ($SiCH_2CH_2S$), 28.4 ($SCH_2CH_2NCH_3$ and SCH_2CH_2O), 30.7 (SCH_2CH_2NH), 39.2 (OCH_2CH_2NH), 44.0 (NCH_3), 58.9 ($SiCH_2CH_2NCH_3$), 70.4 **(**OCH_2), 113.6 (CAr, *orto-OH, orto-CH=CH*), 115.1 (CAr, *meta-CH=CH*), 117.1 (PhCH=CH(CO)NH*)*, 120.8, (CAr, *orto-CH=CH*), 140.8 (PhCH=CH(CO)NH), not observed (Cipso), not observed (NHC=O). **Elemental Analysis (%):** Calc for $C_{225}H_{458}N_8O_{80}S_8Si_5$ (4953.02 g/mol). C, 54.56; H, 9.32; N, 2.26; S, 5.18. Exp.: C, 54.51; H, 8.727; N, 2.223; S, 5.631.

2.1.4. Synthesis of G_2-[(S-PEG-NH(CO)CH=CHCH$_2$Ph(OH)$_2$)$_2$(S-N(CH$_3$)$_2$)$_6$] (14)

Dendrimer **14** was again prepared by the same method as **11** using the following reagents: caffeic acid (33.73 mg, 0.187 mM), EDCI·HCl (35.81 mg, 0.187 mM), HOBt (24.92 mg, 0.187 mM), G_2-[(S-PEG-NH$_2$)$_2$(S-N(CH$_3$)$_2$)$_6$] (**10**) (381.13 mg, 0.046 mM) and Na_2CO_3 (35.72 mg, 0.337 mM). Compound **13** was obtained as a brown solid (178.3 mg, 48%).

^{1}H NMR (CD_3OD):δ (ppm) 0.08 (s, 12H, $SiCH_3$), 0.66 (m, 8H, $SiCH_2CH_2CH_2Si$), 0.72 (m, 8H, $SiCH_2CH_2CH_2Si$), 0.95 (m, 16H, $SiCH_2CH_2S$), 1.42 (m, 8H, $SiCH_2CH_2CH_2Si$), 2.28 (s, 36H, NCH_3), 2.55 (m, 12H, $SCH_2CH_2NCH_3$), 2.60–2.75 (m, overlapping of signals, 32H, $SiCH_2CH_2S$, $SCH_2CH_2NCH_3$ and SCH_2CH_2O), 3.49 (m, 4H, O-CH_2CH_2NH), 3.55–3.71 (m, 616H, OCH_2), 6.41 (d, 2H, $^3J_{(H—H)}$ = 15.7 Hz, PhCH=CH(CO)NH), 6.76 (d, 2H, $^3J_{(H—H)}$ = 8.2 Hz, $1H_{Ar}$, *meta-CH=CH*), 6.90 (dd, 2H, $^3J_{(H—H)}$ = 8.2 Hz, $^5J_{(H—H)}$ = 2.1 Hz, $2H_{Ar}$, *ortho-CH=CH*), 7.01 (d, 2H, $^5J_{(H—H)}$ = 2.1 Hz, $2H_{Ar}$, *ortho-CH=CH, ortho-OH*), 7.40 (d, 2H, $^3J_{(H—H)}$ = 15.7 Hz, PhCH=CH(CO)NH). **^{13}C {^{1}H}-NMR (CD_3OD):** δ (ppm) -6.1 $SiCH_3$), 14.3 ($SiCH_2CH_2S$), 17.1 ($SiCH_2CH_2CH_2Si$), 17.9 ($SiCH_2CH_2CH_2Si$), 18.2 ($SiCH_2CH_2CH_2Si$), 27.0 ($SiCH_2CH_2S$), 28.4 ($SCH_2CH_2NCH_3$ and SCH_2CH_2O), 30.7 (SCH_2CH_2NH), 38.8 (OCH_2CH_2NH), 43.8 (NCH_3), 58.9 ($SiCH_2CH_2NCH_3$), 70.0 **(**OCH_2), 113.3 (CAr, *orto-OH, orto-CH=CH*), 115.9 (CAr, *meta-CH=CH*), 116.8 (PhCH=CH(CO)NH), 120.5, (CAr, *orto-CH=CH*), 139.7 (PhCH=CH(CO)NH), not observed (Cipso), not observed (NHC=O). **Elemental Analysis (%):** Calc for $C_{386}H_{768}N_8O_{160}S_8Si_5$ (8479.19 g/mol). C, 54.68; H, 9.13; N, 1.32; S, 3.02. Exp.: C, 54.58; H, 8.672; N, 1.54; S, 2.99.

2.1.5. Synthesis of G_2-[(S-(CH$_2$)$_2$NH(CO)CH=CHCH$_2$Ph(OH)$_2$)(S-N(CH$_3$)$_3$Cl)$_7$] (15)

Methyl iodide (MeI) (0.15 mL, 2.443 mM) was added over a tetrahydrofuran (THF) solution of dendrimer G_2-[(S-(CH$_2$)$_2$NH(CO)CH=CHCH$_2$Ph(OH)$_2$)(S-N(CH$_3$)$_2$)$_7$] (**11**) (453 mg, 0.290 mM) and stirred for 24 h. The volatiles were removed under vacuum, the remaining solid was dissolved in water, and the iodide ion was exchanged for chloride through amberlite IRA—Cl. After the solvents were evaporated the solid obtained was washed several times with Et_2O and dried under vacuum, leaving compound **15** as a brown solid in a moderate yield (376.2 mg; 67.6%).

^{1}H NMR (CD_3OD):δ (ppm) 0.12 (s, 12H, $SiCH_3$), 0.67 (m, overlapping signals, 16H, $SiCH_2CH_2CH_2Si$), 0.98 (m, 16H, $SiCH_2CH_2S$), 1.42 (m, 8H, $SiCH_2CH_2CH_2Si$), 2.74 (m, 8H, $SiCH_2CH_2S$), 3.00 (m, 16H, $SCH_2CH_2N^+CH_3$ and SCH_2CH_2NH), 3.22 (broad s, 63H, N^+CH_3), 3.53–3.83 (m, overlapping signals, 16H, $SCH_2CH_2N^+CH_3$ and SCH_2CH_2NH), 7.36 (broad m, 1H, PhCH=CH(CO)NH), 7.47–7.68 (C_6H_4)), 7.98 (broad m, 1H, PhCH=CH(CO)NH). **Elemental Analysis (%):** Calc for $C_{78}H_{171}Cl_7N_8O_3S_8Si_5$ (1914.33 g/mol). C, 48.94; H, 9.00; N, 5.85; Exp.: C, 44.64; H, 8.430; N, 5.191.

2.1.6. Synthesis of G_2-[(S-(CH$_2$)$_2$NH(CO)CH=CHCH$_2$Ph(OH)$_2$)$_2$(S-N(CH$_3$)Cl)$_6$] (16)

Dendrimer **16** was prepared by the same method as 15 using the following reagents: MeI (0.026 mL, 0.420 mM); G_2-[(S-(CH$_2$)$_2$NH(CO)CH=CHCH$_2$Ph(OH)$_2$)$_2$(S-N(CH$_3$)$_2$)$_6$] (**12**) (85.5 mg; 0.05 mM). Compound **16** was obtained as a yellow solid (62.83 mg, 62.9%).

^{1}H NMR (CD_3OD):δ (ppm) 0.12 (s, 12H, $SiCH_3$), 0.67 (m, overlapping signals, 16H, $SiCH_2CH_2CH_2Si$), 0.98 (m, 16H, $SiCH_2CH_2S$), 1.42 (m, 8H, $SiCH_2CH_2CH_2Si$), 2.74 (m, 8H, $SiCH_2CH_2S$), 3.00 (m, 16H, $SCH_2CH_2N^+CH_3$ and SCH_2CH_2NH), 3.22 (broad s, 54H, N^+CH_3), 3.53–3.83 (m, overlapping signals, 16H, $SCH_2CH_2N^+CH_3$ and SCH_2CH_2NH), 7.36 (broad m, 2H, PhCH=CH(CO)NH), 7.47–7.68 (C_6H_4)), 7.98 (broad m, 2H, PhCH=CH(CO)NH). **Elemental Analysis (%):** Calc for $C_{80}H_{166}Cl_6N_8O_8S_8Si_5$ (1977.86 g/mol). C, 48.58; H, 8.46; N, 5.67; Exp.: C, 43.82; H, 7.859; N, 6.562.

2.1.7. Synthesis of G_2-[(S-PEG-NH(CO)CH=CHCH$_2$Ph(OH)$_2$)(S-N(CH$_3$)$_3$Cl)$_7$] (17)

Dendrimer **17** was again prepared by the same method as **15** using the following reagents: MeI (0.027 mL, 0.444 mM); G_2-[(S-PEG-NH(CO)CH=CHCH$_2$Ph(OH)$_2$)(S-N(CH$_3$)$_2$)$_7$] (**13**) (262.5 mg; 0.053 mM). Compound **17** was obtained as a yellow solid (110 mg, 42.3%).

^{1}H NMR (CD_3OD):δ (ppm) 0.10 (s, 12H, $SiCH_3$), 0.65 (m, overlapping signals, 16H, $SiCH_2CH_2CH_2Si$), 0.96 (m, 16H, $SiCH_2CH_2S$), 1.42 (m, 8H, $SiCH_2CH_2CH_2Si$), 2.74 (m, 8H, $SiCH_2CH_2S$), 3.00 (m, 32H, $SCH_2CH_2N^+CH_3$, SCH_2CH_2NH and S-CH_2CH_2O), 3.22 (broad s, 63H, N^+CH_3), 3.53–3.83 (m, overlapping signals, 387H, N^+CH_3, $SCH_2CH_2N^+CH_3$, SCH_2CH_2NH, OCH_2), The signal corresponding to aromatic rings not appreciated **Elemental Analysis (%):** Calc for $C_{232}H_{479}Cl_7N_8O_{80}S_8Si_5$ (5306.42 g/mol). C, 52.51; H, 9.10; N, 2.11. Exp.: C,52.99; H,9.60; N, 2.45.

2.1.8. Synthesis of G_2-[(S-PEG-NH(CO)CH=CHCH$_2$Ph(OH)$_2$)$_2$(S-N(CH$_3$)$_3$Cl)$_6$] (18)

Dendrimer **18** was prepared by the same method using the following reagents: MeI (55.8 mg, 0.024 mL); G_2-[(S-PEG-NH(CO)CH=CHCH$_2$Ph(OH)$_2$)$_2$(S-N(CH$_3$)$_2$)$_6$] (14) (371.3 mg; 0.046 mM). Compound **18** was obtained as a pallid yellow solid (211.5 mg, 51.4%).

^{1}H NMR (CD_3OD):δ (ppm) 0.99 (s, 12H, $SiCH_3$), 0.66 (m, overlapping signals, 16H, $SiCH_2CH_2CH_2Si$), 0.96 (m, 16H, $SiCH_2CH_2S$), 1.42 (m, 8H, $SiCH_2CH_2CH_2Si$), 2.74 (m, 8H, $SiCH_2CH_2S$), 3.00 (m, 32H, $SCH_2CH_2N^+CH_3$, SCH_2CH_2NH and S-CH_2CH_2O), 3.22 (broad s, 54H, N^+CH_3), 3.53–3.83 (m, overlapping signals, 677H, N^+CH_3, $SCH_2CH_2N^+CH_3$, SCH_2CH_2NH, OCH_2), The signal corresponding to aromatic rings not appreciated). The signal corresponding to aromatic rings not appreciated. **Elemental Analysis (%):** Calc for $C_{392}H_{786}Cl_6N_8O_{160}S_8Si_5$ (8782.10 g/mol). C, 53.61; H, 9.02; N, 1.28. Exp.: C, 54.01; H,9.33; N,2.92.

2.2. Hydrodynamic diameter, zeta potential and transmission Electron microscopy

The hydrodynamic diameters of the polyphenolic dendrimers were measured by dynamic light-scattering (DLS) using a photon correlation spectrometer (Zetasizer Nano-ZS, Malvern Instruments, UK) in DTS0012 plastic cells (Malvern), in 10 mM Na-phosphate buffer (disodium hydrogen phosphate & monosodium phosphate, 4:1), pH 7.4 at 25 °C. Dendrimer concentration was 10 μM. To analyze the surface charge parameters, the zeta potential was measured in 10 mM Na-phosphate buffer (disodium hydrogen phosphate & monosodium phosphate, 4:1), pH 7.4 at 25 °C using the same Malvern spectrometer. The final dendrimer concentration in the samples was 10 μM. The zeta potential was calculated directly from the Helmholtz-Smoluchowski Eq. [45]. Malvern software was used for data analysis. Three separate experiments were conducted, each in seven replicates.

Dendrimer morphology and size were examined by transmission electron microscopy (TEM). Dendrimer samples (10 μL), 1 mM in Na-phosphate buffer (PB), were placed on 200 mesh copper grids with a carbon surface, stained with 2% uranyl acetate for 20 min, washed with deionized water and dried at room temperature. Images were obtained using a JEOL1010 transmission electron microscope (JEOL, Tokyo, Japan).

2.3. Cell viability assay

To evaluate the cytotoxic effects of dendrimers, BJ (normal human fibroblasts) and A549 (cancer human alveolar basal epithelial cells) were used in RPMI 1640 and DMEM (Gibco), respectively, supplemented with 10% bovine serum (FBS) and 1% antibiotics (penicillin/streptomycin, 1:1) at 37 °C in an atmosphere of 5% CO_2 and 95% humidity. The Colorimetric cell viability assay (MTT) assay was used to determine percentage cell viability. Cells were seeded in a 96-well plate (10,000 cells/well) and incubated (24 h, 37 °C, 5% CO_2), and dendrimers (12.5–100 μM) were added to the wells and incubated for 24 h. MTT (0.5 mg/mL per well) was added for 2 h, and then 100 μL DMSO was added to each well to dissolve the formazan crystals. Sample absorbance was measured at λ = 580 nm (background correction at 720 nm) using a multiwell plate reader (BioTek PowerWave HT, BioTek Instruments, Inc. Winooski, VT, USA). The percentage cell viability was calculated by the formula:

$$\text{Viability}\ [\%] = \frac{A_{sample} \times 100}{A_{control}}$$

2.4. Oxidative stress: Antioxidant and antiradical activity

2.4.1. Free radical scavenging activity

The free radical scavenging activity of the dendrimers was measured using the free radical DPPH (2,2′-diphenyl-1-picrylhydrazyl); antioxidants change the colour of a DPPH solution from purple to yellow. Aliquots of 0.25 mM DPPH in ethanol (180 μL) were mixed with (20 μL) dendrimer solutions, to the final concentrations of dendrimers 12.5–100 μM and incubated in the dark at room temperature for 30 min. The absorbance was measured at λ = 517 nm using a Jasco V-650 spectrophotometer. The scavenging activity was determined from the percentage decrease in DPPH absorbance according to the formula:

$$DPPH_{inhibition}\ [\%] = 100(A_0 - A_P)/A_0.$$

where A_0 is the absorbance of the DPPH solution and A_P is the absorbance of DPPH samples after incubation with dendrimers.

2.4.2. Ferric Reducing Antioxidant Power (FRAP) assay presented as Trolox Equivalent Antioxidant Capacity (TEAC)

Antioxidant activity was also measured by the reduction of Fe^{3+} to Fe^{2+} in the presence of TPTZ (2,4,6-tripyridyl-striazine), forming an intense blue Fe^{+2}–TPTZ complex with maximum absorption at 593 nm. Aliquots of FRAP solution (180 μL) were placed in 96 well plates and 20 μL of 10–100 μM dendrimer in methanol was added. After incubation in the dark at room temperature for 30 min, the absorbance at λ = 517 nm was measured using a microplate reader (EpochTM, BioTek Instruments, Winooski, VT, USA). The antioxidant activity of FRAP was expressed as TEAC (Trolox Equivalent Antioxidant Capacity) using the standard curve (Figure Si.22) prepared with a methanol solution of Trolox at concentrations ranging from 10 to 100 μM. The results are presented as μM trolox/μM compound. All tests were performed in triplicate and methanol was used as control.

2.4.3. Lipid peroxidation

The level of lipid peroxidation in erythrocyte membranes in the presence of polyphenolic dendrimers was determined using the fluorescent probe 4,4-difluoro-5-(4-phenyl-1,3-butadienyl)-4-bora-3a,4a-diaza-s-indacene-3-un-decanoic acid (BODIPY581/591). Lipid peroxidation was induced by adding α,α'-Azodiisobutyramidine dihydrochloride (AAPH) to a suspension of human erythrocyte membranes. Red blood cells were haemolysed in PB and centrifuged at 15,000 ×*g* for 15 min at 4 °C. The membranes were washed several times with dilute Na-phosphate buffer and incubated for 60 min with 12.5–100 μM dendrimers and 50 mM AAPH, with gentle vortexing. BODIPY581/591 (2.5 μM) was added to the samples. Fluorescence was measured at excitation λ = 485 nm and emission λ = 530 nm wavelengths using a multiwell plate reader (BioTek PowerWave HT, BioTek Instruments, Inc. Winooski, VT, USA). The results were calculated as:

$$\text{Lipid peroxidation}\ [\%] = \frac{A_s \times 100}{A_{0.}}$$

Where: A_0 is fluorescence of the sample incubated with AAPH; A_s fluorescence of samples with AAPH and dendrimers.

2.4.4. AAPH-induced haemolysis

Erythrocytes isolated as described above (hematocrit 7%) were incubated with PBS (control) and preincubated with dendrimers at 12.5–100 μM and 50 mM AAPH in PBS. The mixtures were gently shaken and incubated for 3 h at 37 °C. PBS was added and the samples were centrifuged at 3000 rpm for 10 min at room temperature. The absorbance of the supernatant was determined at λ = 535 nm using a Jasco V-650 spectrophotometer. Reference values were measured using the same volume of erythrocytes with AAPH but without dendrimers. The percentage of AAPH-induced haemolysis was calculated from the formula:

$$H\ [\%] = \frac{A_{sample} \times 100}{A_{control\ positive}}$$

2.4.5. Inhibition of cellular reactive oxygen species (ROS) production

The ability to decrease the level of cellular reactive oxygen species (ROS) was tested using BJ cells seeded on black plates and treated with 12.5–100 μM dendrimers. Oxidative stress and ROS production were induced by adding 50 mM AAPH. To measure the ROS level, non-fluorescent 2′,7′-dichlorofluorescindiacetate (H_2DCF-DA) (10 μM) was added. Under oxidative stress, H_2DCF-DA is converted to highly fluorescent 2′,7′-dichlorofluorescein (DCF). After 30 min. Incubation, DCF fluorescence was measured at $\lambda_{exc} = 485$ nm and $\lambda_{em} = 530$ nm in a multiwell plate reader (BioTek PowerWave HT, BioTek Instruments, Inc. Winooski, VT, USA).

Confocal microscopy was used to visualize the ability of dendrimers to decrease the level of ROS in BJ cells. Cells were seeded on labtec plates and treated with dendrimers at 50 μM. Oxidative stress was induced by adding 50 mM AAPH, followed by the probe H_2DCF-DA (10 μM). Microphotographs were taken at $\lambda_{em} = 490$ nm, $\lambda_{em} = 527$ nm using a confocal microscope (Leica TCS LSI, Leica Microsystems, Frankfurt, Germany) with a 63×/1.40 (HC PL APO CS2, Leica Microsystems) objective. Leica Application Suite X software (LAS X, Leica Microsystems, Frankfurt, Germany) was used to obtain and analyze the images.

2.5. Statistical analysis

A *t*-test was used to compare two groups of samples. For more than two groups the Kruskal-Wallis test was used.

3. Results

3.1. Synthesis and characterization

To prepare dendritic systems with a caffeic acid and $-NMe_3^+$ moieties on the surface, we used a random approach, starting from spherical carbosilane dendrimers with vinyl groups at the periphery non-soluble in water. The vinyl groups allowed primary amino groups to be introduced by thiol-ene click chemistry. These groups are necessary for attaching caffeic acid to the dendritic surface by straightforward amidation (Fig. 2) [46].

In this work, heterofunctionalized dendrimers were obtained using two types of thiol derivative, which allowed the primary amino groups necessary for the subsequent amidation to be introduced. Following the methods in the literature [47], the reaction of vinyl dendrimer G2 (vinil) 8 (**I**) with one or two equivalents of (i) cysteamine hydrochloride HS $(CH_2)_2NH_3Cl$ or (ii) a commercial thiol HS-PEG-NH_2·HCl (MW = 3.5 kDa) generated the heterofunctionalized derivatives G_2[(vinyl)n (NH_2 . HCl)m] (*n* = 7, m = 1 (**II**); *n* = 6, m = 2 (**III**)) and G_2[(Vinyl)n(PEG-NH_2.HCl)m] (n = 7, m = 1 (**1**); n = 6, m = 2 (**2**)). ^{1}H NMR spectra confirmed the introduction of the new chain in each case. Compounds **I** and **II** showed the methylene group resonances of the new chain Si $(CH_2)_2$S at δ ca. 2.57 for the single bond to the sulphur atom, and 0.99 ppm for the methylene group next to the silicon atom, respectively. They also showed the resonances of polyethylene glycol methylene groups at 3.62 ppm (Fig. 3). Likewise, ^{1}H NMR was used to determine the number of amino groups in the dendritic system. For this, the integral relationship between the signals corresponding to the methylene group bonded to the sulphur atom (Si$(CH_2)_2$S) of the newly-introduced chain and the resonances of the vinyl groups was used [47]. The remaining vinyl groups were functionalized with an excess of the thiol HS $(CH_2)_2NMe_2$·HCl, producing the systems G_2[(NMe_2•HCl)n(NH_2•HCl)m] (*n* = 7, m = 1 (**3**); *n* = 6, m = 2 (**4**)) and G2[(NMe_2HCl)n(PEG-NH_2.HCl) m] (*n* = 7, m = 1 (**5**); *n* = 6, m = 2 (**6**)). Again, ^{1}H NMR spectra confirmed the total functionalization of the remaining vinyl groups by the disappearance of their corresponding resonances and the appearance of a new signal at δ ca. 2.91 belonging to the methyl groups bound to the nitrogen of the new chain. The neutralization of cationic compounds **3**–**6** with Na_2CO_3 allowed the corresponding dendritic derivatives with amino group G_2[(NMe_2)n(NH_2)m] ((*n* = 7, m = 1 (**7**); *n* = 6, m = 2 (**8**)) and G2[(NMe_2)n(PEG-NH_2)m] (n = 7, m = 1 (**9**); n = 6, m = 2 (**10**)) to be obtained. Neutralization of the amino groups was corroborated by ^{1}H NMR: the signal corresponding to methyl groups bound to the nitrogen atom was displaced from 2.91 to 2.21 ppm. Once obtained compounds **7**–**10** with two different terminal amine groups, the formation of an amide bond by condensation of a carboxylic acid present in caffeic acid and an primary amine located in the dendritic branched using N-(3-dimethylaminopropyl)-N′-ethylcarbodiimide hydrochloride (EDCI·HCl) and 1-hydroxybenzotriazole (HOBt) as coupling reagents, which prevent the acid-base reaction and makes the carboxylic acid susceptible to a nucleophilic attack, allowing the obtention of the heterofunctionalized dendrimers G_2[(NMe_2)n(NH-CA)m] (*n* = 7, m = 1 (**11**); *n* = 6, m = 2 (**12**)) and G_2[(NMe_2)n(PEG-NH-CA)m] (n = 7, m = 1 (**13**); n = 6, m = 2 (**14**)). Amide formation was confirmed by ^{1}H and ^{13}C NMR; the spectra showed the displacement of the methylene group bound to the amide fragment from 2.99 (-C$H_2$$NH_2$) to 3.40 ppm (-C(*O*) NHCH_2) in ^{1}H NMR and from 28.2 (-CH_2NH_2) to 39 ppm (-C(*O*)NHCH_2-) in ^{13}C NMR. Furthermore, signals assigned to the alkene fragment at 6.45 and 7.42 ppm in ^{1}H NMR and 118.5 and 142.2 ppm in ^{13}C NMR were observed, along with a set of signals belonging to aromatic protons at 6.80, 6.95, and 7.05 ppm in ^{1}H NMR and between 115.0 and 148.9 ppm in ^{13}C NMR (Figs. 4 and 5). Finally, the amino groups present in the dendritic structure of compounds **11**–**14** were quaternized with methyl iodide in order to obtain water soluble macromolecules. Afterwards, iodide ions were exchanged for chloride through amberlite IRA-Cl and the reaction mixtures were purified by size exclusion chromatography allowing polyphenolic carbosilane dendrimers G_2[(NMe_3Cl)n(NH-CA) m] (*n* = 7, m = 1 (**15**); *n* = 6, m = 2 (**16**)) and G_2[(NMe_3Cl)n(PEG-NH-CA)m] (n = 7, m = 1 (**17**); n = 6, m = 2 (**18**)) to be obtained as brown solids in moderate yields and soluble in water. The ^{1}H and ^{13}C NMR spectra of ionic heterofunzionalized dendrimers **15**–**18** showed

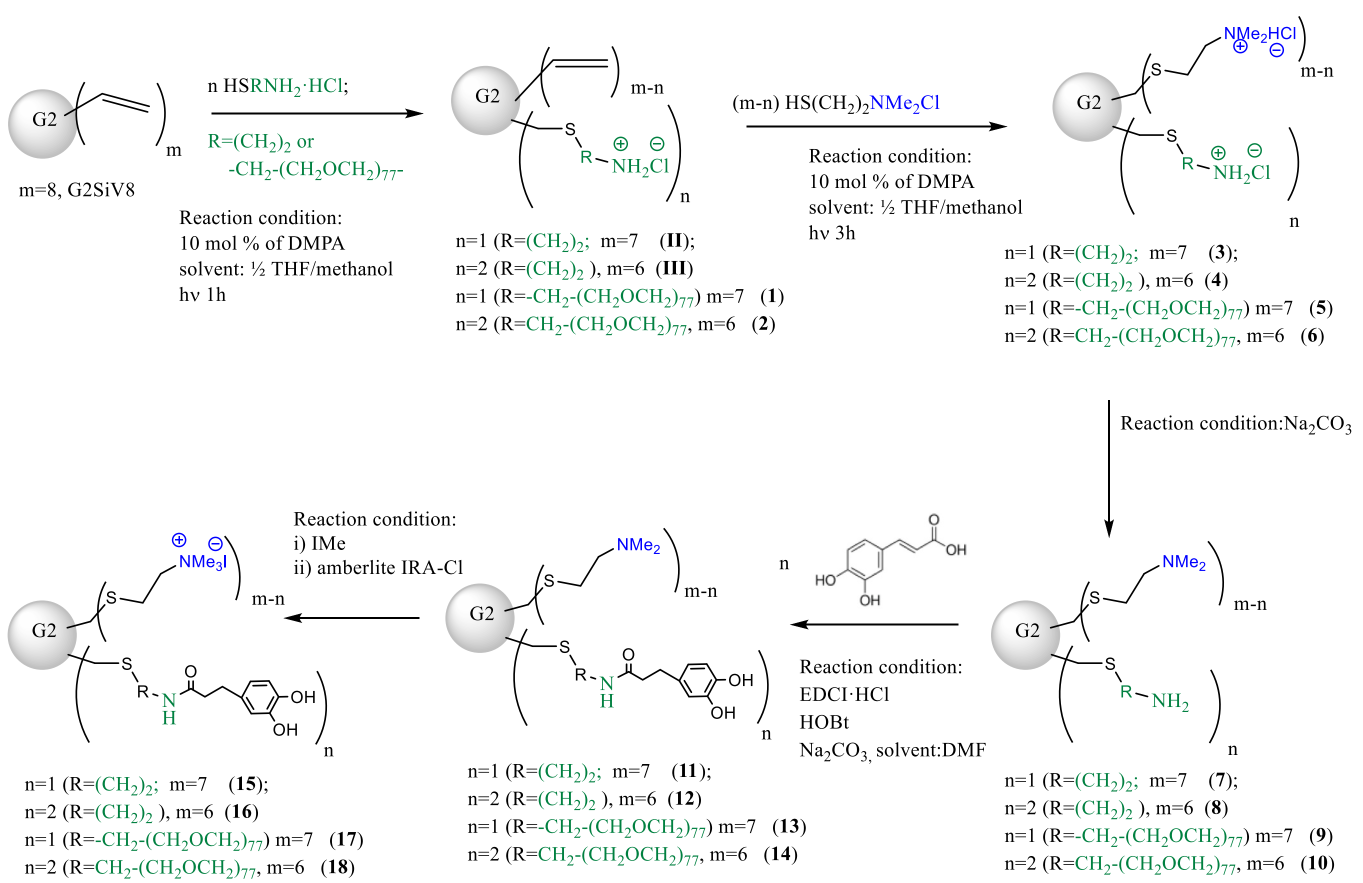

Fig. 2. Schematic representation of the synthetic steps of polyphenolic dendrimers.

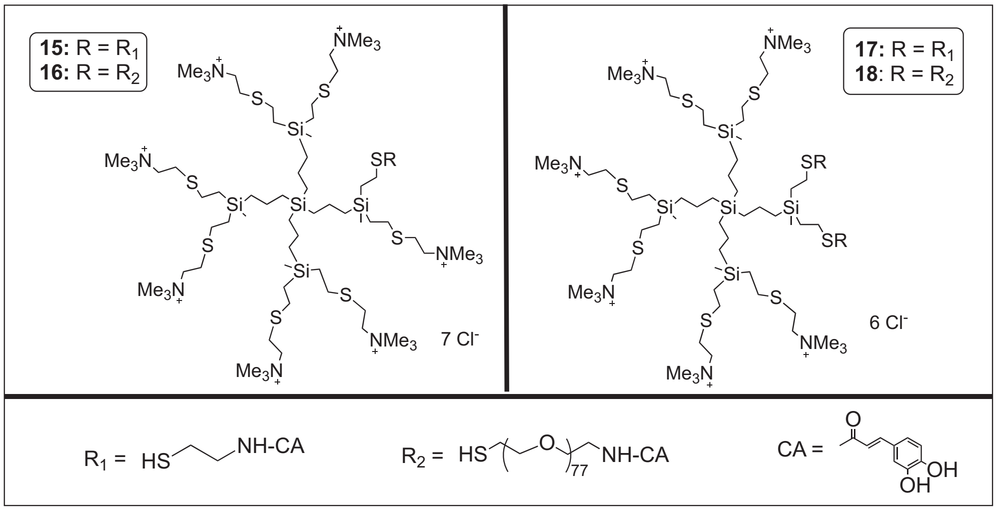

Fig. 3. Proposed structure of heterofunctionalized polyphenolic carbosilane dendrimers.

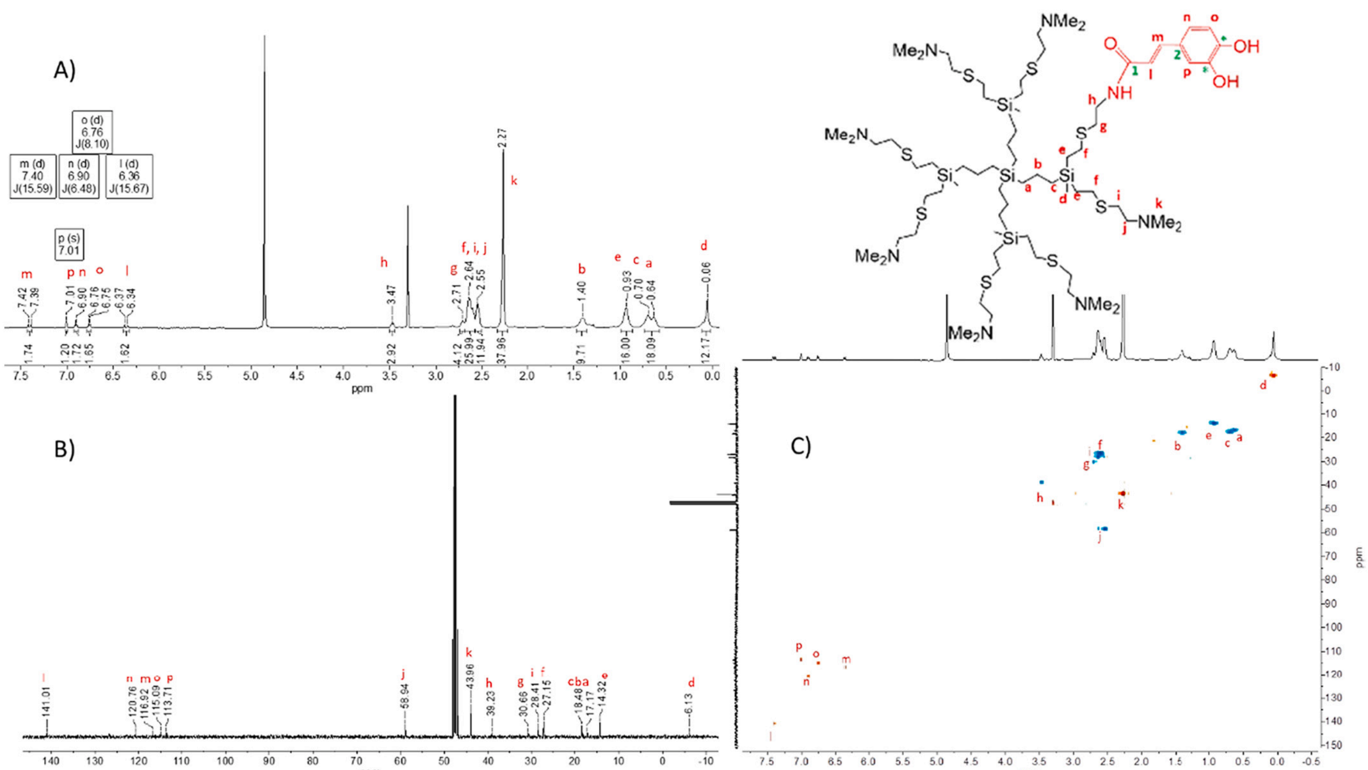

Fig. 4. NMR spectra in CD_3OD of compound $G_2[(NMe_2)_7(NH\text{-}CA)]$ (**11**): (A) ^1H NMR, (B) ^{13}C NMR, and (C) {^1H–^{13}C}-HSQC-2D-NMR (500 MHz, CD_3OD) (d, doublet; dd, doublet of doublets).

resonance patterns identical to those of their neutral precursors **11**–**14** for the carbosilane framework; quaternization of the amine groups revealed a deshelling of about Δd = 1 ppm with respect to the neutral derivatives in the chemical shifts of the signal attributed to the outer chain $S(CH_2)_2N$ and the methyl group NMe_3 that appears at 3.00 ppm.

Please see Supplementary Material Information for more synthesis details, including figs. S1-S23.

3.2. Biophysical characterization

3.2.1. Average size, surface charge and polydispersity index

To characterize the new compounds, their mean diameter, zeta potential and polydispersity index were measured. The average dendrimer sizes are shown in Fig. 6A. The histograms show the percentage distribution of nanoparticle numbers, indicating their hydrodynamic diameter. The dendrimer **15** formulations ranged in diameter from 50 to 200 nm and other dendrimers from 100 to 800 nm. The average dendrimer sizes were: $G_2[(NMe_3Cl)_7(NH\text{-}CA)]$ (**15**), 215.6 ± 8.6 nm; $G_2[(NMe_3Cl)_6(NH\text{-}CA)_2]$ (**16**), 440.2 ± 20.0 nm; $G_2[(NMe_3Cl)_7(PEG\text{-}NH\text{-}CA)]$ (**17**), 460.8 ± 23.3 nm; $G_2[(NMe_3Cl)_6(PEG\text{-}NH\text{-}CA)_2]$ (**18**), 476.4 ± 12.9 nm. The polydispersity index (PDI), a parameter indicating nanoparticle heterogeneity, is shown in Fig. 6D. The PDIs of the polyphenolic dendrimers were: **15**: 0.45 ± 0.03, **16**: 0.6 ± 0.02, **17**: 0.46 ± 0.01, **18**:0.44 ± 0.01.

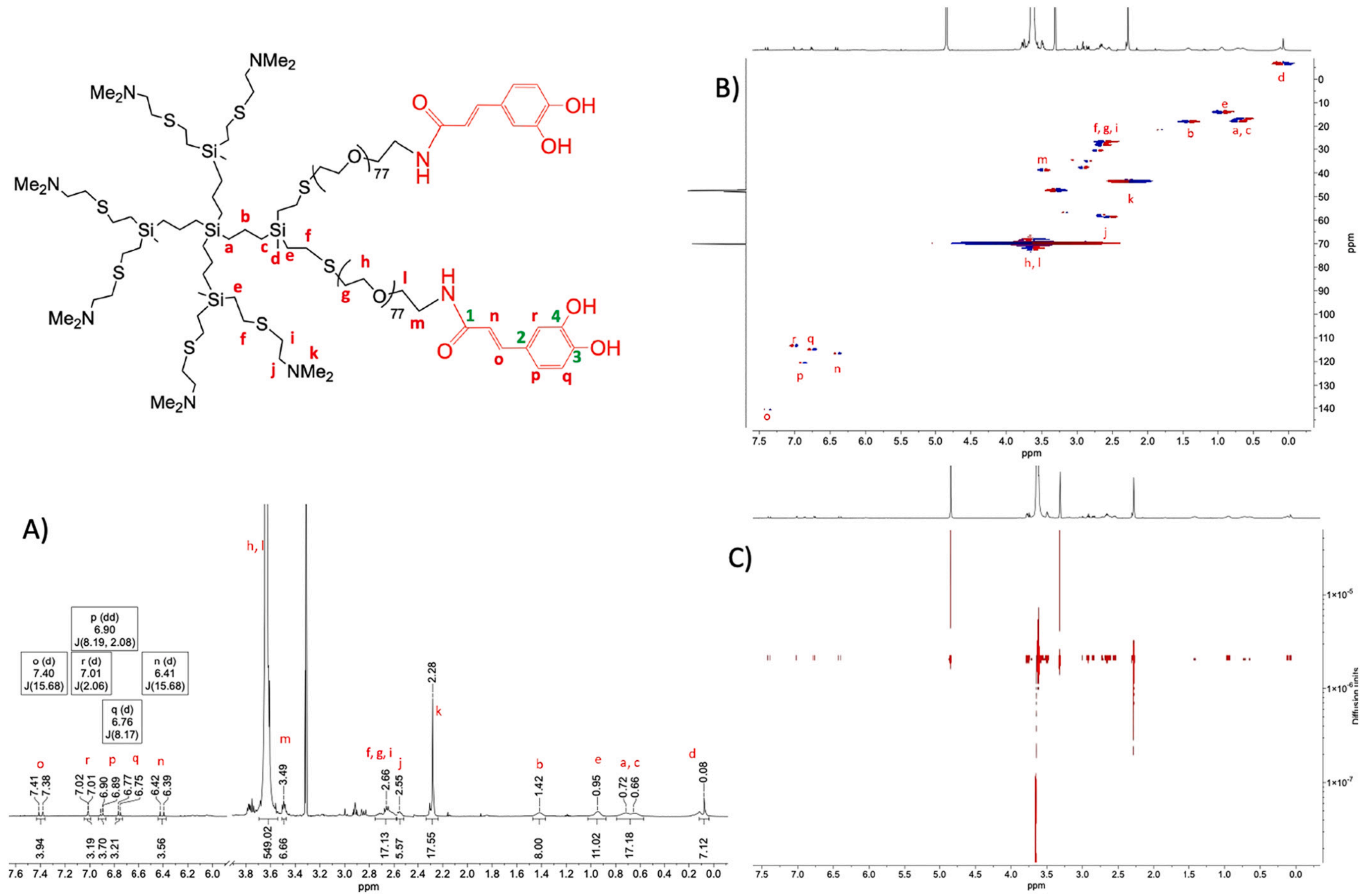

Fig. 5. NMR spectra in CD_3OD of compound $G_2[(NMe_2)_6(PEG\text{-}NH\text{-}CA)_2]$ (**14**): (A) ^1H NMR, (B) {^1H–^{13}C}-HSQC-2D-NMR, and (C) ^1H-DOSY-2D-NMR (d, doublet; dd, doublet of doublets).

The zeta potential values are presented in Fig. 6C. All nanoparticles were positively charged. The PEG-free dendrimers had the highest zeta potentials: **15**, 18.6 ± 0.3 mV and **16**, 21.1 ± 0.5 mV. Dendrimers with PEG anchored in their scaffolds had lower zeta potentials: **17**, 2.8 ± 0.1 mV and **18**, 2.9 ± 0.05 mV.

3.2.2. Transmission Electron Microscopy (TEM)

To characterize dendrimer morphology and size, TEM microimages were examined (Fig. 6B). Nanoparticles were visible as single dots and they were smaller than 5 nm. Images show that dendrimers with PEG (**17**, **18**) were bigger than PEG-free dendrimers (**15**, **16**). Substances with low electron density were observed between the nanoparticles. This could explain the big differences in DLS and TEM results. Perhaps dendrimers can form structures containing several molecules attached to each other, which are bigger than a single dendrimer molecule and were probably detected with the Zetasizer spectrometer.

3.3. Dendrimer cytotoxicity

The cytotoxic effect of polyphenol dendrimers towards BJ (normal) and A549 (cancer) cells was evaluated after 24 h incubation (Fig. 7). All dendrimers had relatively low cytotoxicity against both cell lines at 12.5–25 μM; the cytotoxic effect on BJ cells was more pronounced. For A549 cells, the most cytotoxic dendrimer was $G_2[(NMe_3Cl)_7(PEG\text{-}NH\text{-}CA)]$ (**17**), which at 100 μM decreased cell viability up to 77% vs control. For BJ cells, dendrimer **17** had similar values at all concentrations tested, the most cytotoxic being PEG-free dendrimer **15** at 50–100 μM. Dendrimer $G_2[(NMe_3Cl)_6(PEG\text{-}NH\text{-}CA)_2]$ (**18**) had similar tendency and decreased the viability of BJ cells up to 50–55% of control.

3.4. Antioxidant activity

3.4.1. DPPH scavenging activity

The ability of dendrimers to scavenge free radicals was studied using the DPPH free radical assay. Incubation of dendrimers with ethanolic solutions of DPPH significantly reduced its light absorbance in a concentration-dependent manner (Fig. 8A).

The effectiveness of dendrimers for free radical scavenging was compared with the antioxidants melatonin, ascorbic acid and caffeic acid. Melatonin had the lowest DPPH radical scavenging activity; caffeic acid was most effective. At the highest concentration, its efficiency reached 87.5 ± 1.1%. The effect of dendrimers was slightly lower than that of caffeic acid, but comparable. The dendrimers at 100 μM showed the highest antiradical activities: PD PEG-CC: 71.7 ± 5.1%, PD PEG—C: 73.9 ± 4.3%, PD-CC: 76.8 ± 5.5%, and PD-C: 78.0 ± 5.7%. The scavenging parameters of ascorbic acid and melatonin at the same concentration were 70.4 ± 16.9% and 14.5 ± 5.1%, respectively.

3.4.2. FRAP assay

This involves the use of a metal complex and can reflect the antioxidant potential of ligands through the reduction of ferric iron, Fe^{3+} to ferrous iron, Fe^{2+}. The Trolox equivalent antioxidant capacity (TEAC) of compounds was established for this assay. The TEAC assay compared the highest mean antioxidant capacity of compounds **15–18** with the standard antioxidant Trolox (Fig. 8B). Dendrimer **18,** with two PEG-caffeic acid moieties, showed the highest antioxidant effect, even higher than free caffeic acid. Other dendrimers were generally less effective, but comparable with caffeic acid. The FRAP assay results presented as Trolox equivalent antioxidant capacity were similar to the DPPH results;

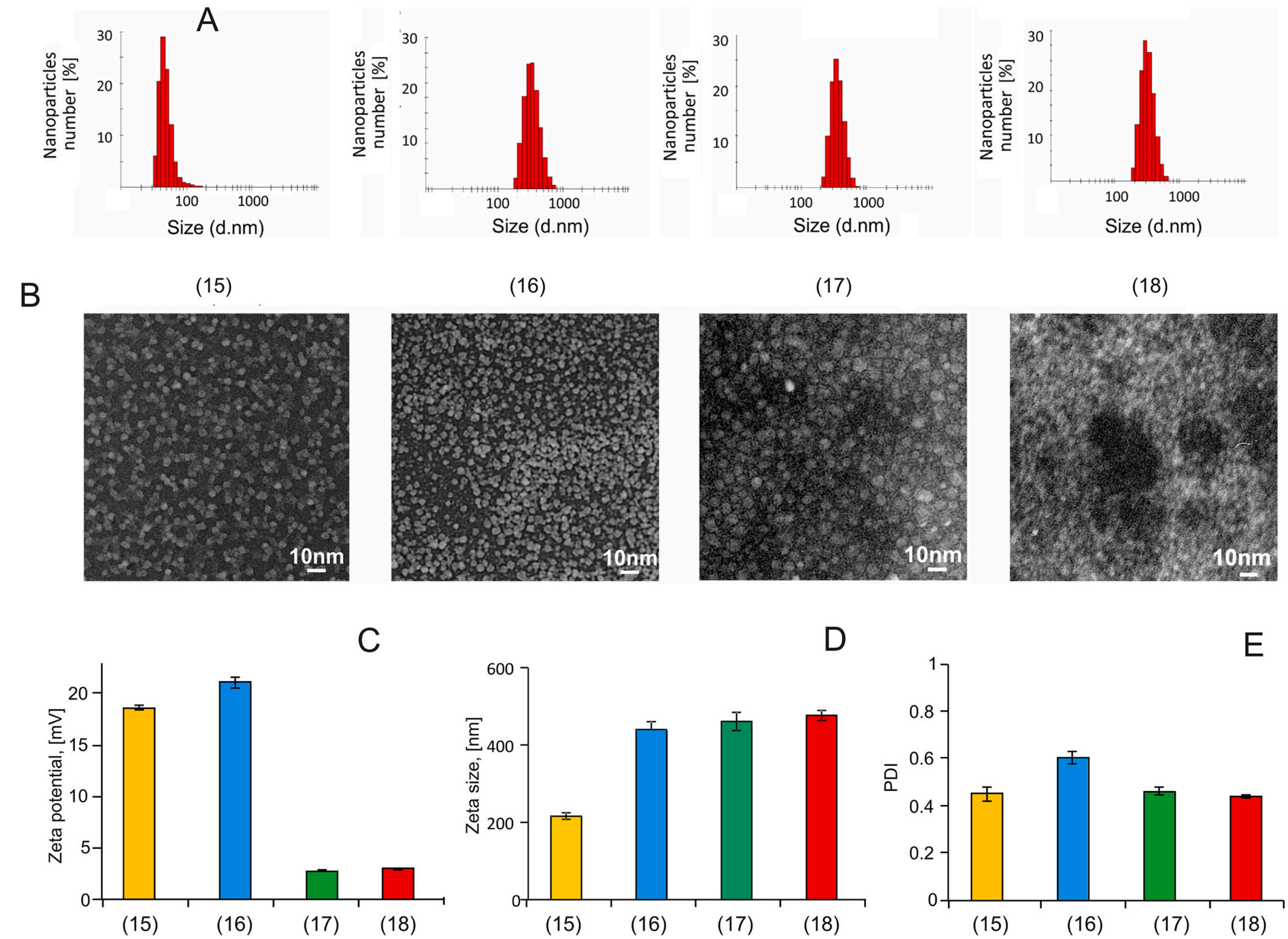

Fig. 6. (A) - Average hydrodynamic diameter of dendrimers: $G_2[(NMe_3Cl)_7(NH\text{-}CA)]$ (**15**); $G_2[(NMe_3Cl)_6(NH\text{-}CA)_2]$ (**16**); $G_2[(NMe_3Cl)_7(PEG\text{-}NH\text{-}CA)]$ (**17**) and $G_2[(NMe_3Cl)_6(PEG\text{-}NH\text{-}CA)_2]$ (**18**) shown as percentage of particle numbers; (B) - TEM images showing morphological characteristics of dendrimers. Samples at the concentration of 1 mM for TEM were dissolved in 10 mM Na-phosphate buffer, placed on copper girds with carbon surfaces and dried. Magnification x100,000; Bars = 10 nm. To obtain greater contrast the colours have been inverted. (C) - Zeta potential (D) – Zeta size and (E) -PDI index of 10 μM dendrimers in Na-phosphate buffer, pH 7.4. Bars represent mean ± SE of three separate experiments and each experiment was done in seven replicates.
TEM: transmission electron microscopy; **PDI**: polydispersity index; **SE**: standard errors.

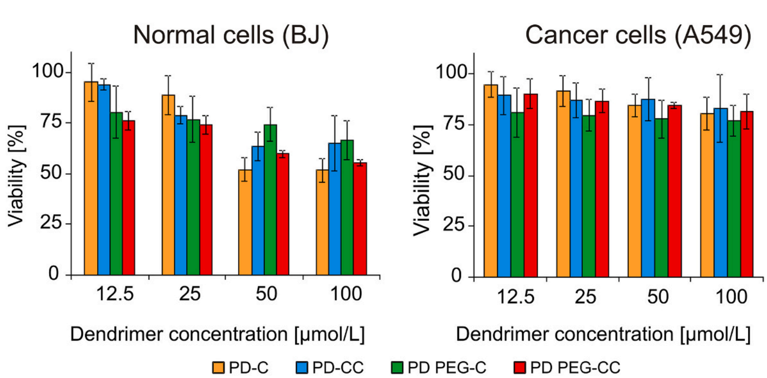

Fig. 7. Viability of BJ (left) and A549 (right) cells in the presence of polyphenolic dendrimers. PBS 10 mM, 10,000 cells/well, MTT 0.5 mg/mL per well, V = 0.2 mL, pH 7.4, incubation time 24 h, $T = 37$ °C, 5% CO_2. Dendrimer concentrations 12.5–100 μM. Values are expressed as mean ± SD ($n = 3$).
BJ: normal human fibroblast cell line; **A549**: human alveolar basal epithelial cancer cell line; **MTT**: 3-[4,5-dimethylthiazol-2-yl]-2,5-diphenyl tetrazolium bromide; **PBS**: phosphate buffered saline; **SD** standard deviation.

all the dendrimers studied showed significant antioxidant potential.

3.4.3. *Lipid peroxidation*

The effect of the dendrimers on the lipid peroxidation level was analyzed by the BODIPY581/591 fluorescence assay. BODIPY581/591 is widely used for measuring lipid peroxidation in various biological membranes. A higher BODIPY581/591 fluorescence intensity indicates more peroxidation. All dendrimers studied reduced the level of AAPH-induced lipid peroxidation; the effect was concentration-dependent (Fig. 8C). The most effective concentration was 100 μM. At 12.5 μM, dendrimers $G_2[(NMe_3Cl)_7(NH\text{-}CA)]$ (**15**) and $G_2[(NMe_3Cl)_6(PEG\text{-}NH\text{-}CA)_2]$ (**18**) conferred the best protection (reduction up to ~30%). In

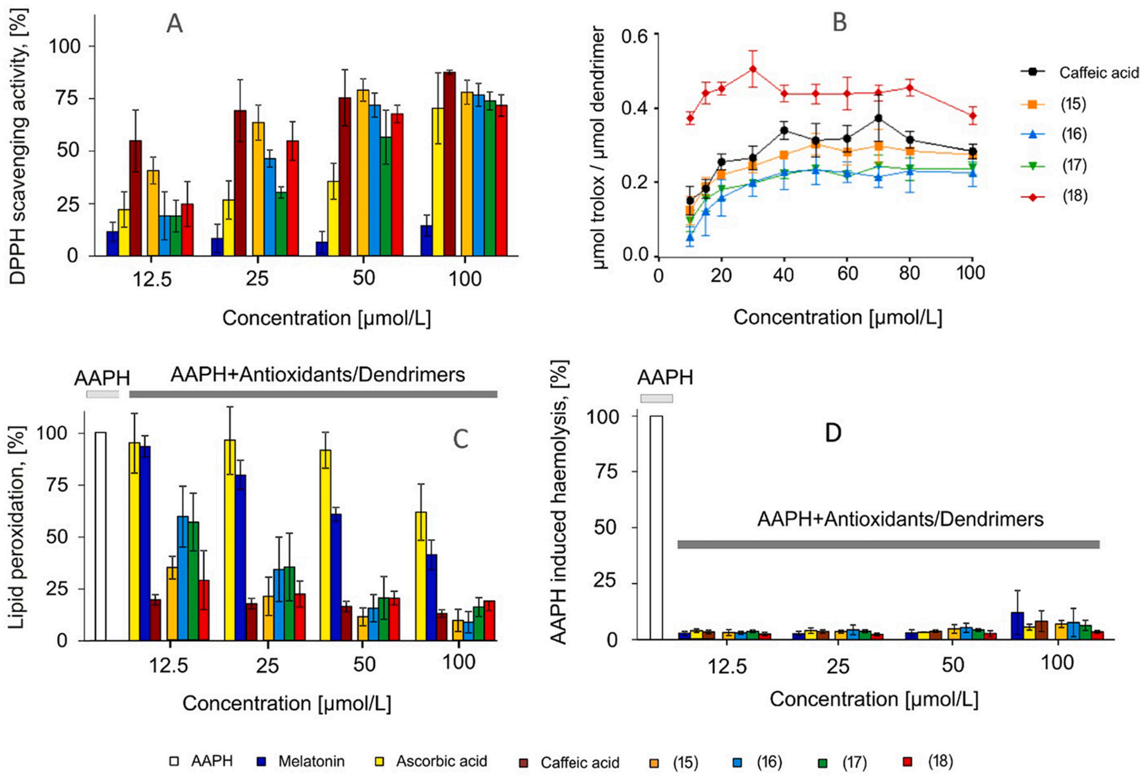

Fig. 8. (A) Percentage of DPPH free radical scavenging by the polyphenolic dendrimers over the concentration range of 12.5–100 μM. Incubation time 30 min. DPPH 0.25 mM, Values are expressed as mean ± SD (n = 3). (B) - Antioxidant behavior of dendrimers estimated by FRAP (Ferric Reducing Antioxidant Power) assay presented as Trolox Equivalent Antioxidant Capacity (TEAC). Values are expressed as mean ± SE (n = 3). (C) - Dendrimers suppress AAPH-induced lipid peroxidation in erythrocyte membranes. PBS 10 mM, pH 7.4, AAPH 50 mM, BODIPY 100 μM, incubation time 60 min, T = 37 °C. Values are expressed as mean ± SD (n = 3). (D) - Antihaemolytic effects of dendrimers on AAPH-induced oxidative haemolysis of human erythrocytes. Hematocrit 7%, PBS buffer 10 mM, pH 7.4, AAPH 50 mM, incubation time 3 h, T = 37 °C. Values are expressed as mean ± SD (n = 3). Dendrimer concentrations ranged from 12.5 to 100 μM. The effects of dendrimers were compared with those of caffeic acid and other antioxidants (except FRAP assay) such as melatonin or ascorbic acid at the same concentrations.
DPPH: 2,2-Diphenyl-1-picrylhydrazyl; **BODIPY®581/1591:** (4,4-difluoro-5-(4-phenyl-1,3-butadienyl)-4-bora-3a, 4a-diaza-s-indacene-3-un-decanoic acid, **FRAP**: Ferric Reducing Antioxidant Power; **TEAC**: Trolox Equivalent Antioxidant Capacity; **AAPH**: 2,2′-azobis(2-amidinopropane) dihydrochloride; PBS: phosphate buffered saline; **SD:** standard deviation.

contrast, at higher concentrations (50–100 μM), dendrimers **15** and **18** provided the most effective protection (up to ~9–8%). Among antioxidants, the most effective was caffeic acid (100 μM), which decreased lipid peroxidation up to 13.1 + 4.96% vs control (AAPH). Melatonin or ascorbic acid, used as controls at 100 μM, showed weaker protective effects than the dendrimers or caffeic acid: 41.3 + 12.8% (melatonin) and 61.7 + 24.4% (ascorbic acid) vs. control.

3.4.4. AAPH-induced haemolysis

The ability of polyphenol dendrimers to protect against AAPH-induced haemolysis was studied. Incubation of human erythrocytes with 50 mM AAPH (oxidant) significantly increased haemolysis. Oxidative AAPH haemolysis reached about 70.7 ± 1.2% vs control after 3 h incubation.

Preincubation of the samples with dendrimers at 12.5–100 μM significantly decreased the level of AAPH-induced hemolysis. After 3 h preincubation at 12.5–50 μM, the haemolysis level decreased up to 5% vs the AAPH control. The slight increase in haemolysis (up to 14%) at 100 μM concentration can be explained by dendrimer haemotoxicity. The reduction of haemolysis by the compounds implies their ability to quench free radicals and increase the antioxidant capacity of erythrocytes, alleviating destructive oxidative haemolysis. The protective effect of dendrimers was comparable with those of ascorbic acid, caffeic acid and melatonin (Fig. 8D).

3.4.5. AAPH-induced ROS production

Since dendrimers demonstrated significant antioxidant and anti-radical activities, we were interested in their ability to protect living cells against increased production of ROS under oxidative stress conditions. All the compounds tested at 50 μM and above inhibited ROS production by the water-soluble free radical generator AAPH in human fibroblasts. The dendrimers were more protective than classical antioxidants such as ascorbic acid or melatonin at the same concentrations (Fig. 9A). This can be explained by the low antioxidant concentrations; their action was not strong enough. On the other hand, caffeic acid caused the most pronounced ROS reduction, decreasing the ROS level up to 30% vs control at 12.5 μM and up to 3% at 25 μM.

Confocal microscopy was also used to visualize the ability of dendrimers to decrease ROS levels. Microimages of BJ cells (Fig. 9B) show decreased fluorescence intensity when dendrimers are present in the cell suspension. The effects of the dendrimers were compared with those of antioxidants. Melatonin (50 μM) did not change the fluorescence intensity of DCF much, indicating weak influence on the cellular ROS level; ascorbic acid had a more pronounced effect (Fig. 9B). Caffeic acid or dendrimers (50 μM) reduced the fluorescence intensity significantly, demonstrating decreased cellular ROS production under oxidative stress conditions.

4. Discussion

The use of dendritic systems in biomedicine is developing

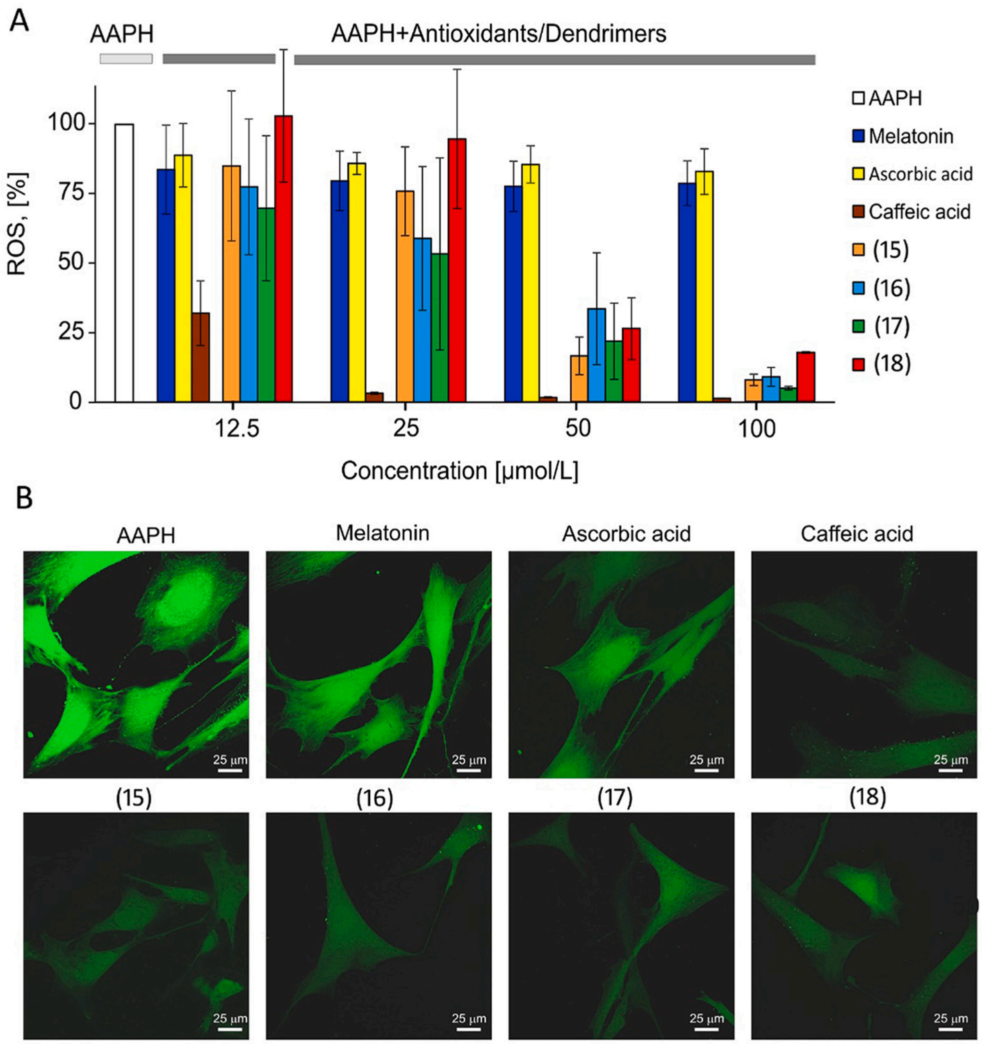

Fig. 9. Effect of polyphenolic dendrimers on AAPH-induced ROS production in BJ cells detected by fluorescence intensity (A) or confocal microscopy (B). PBS 10 mM, pH 7.4, AAPH 50 mM, H_2DCF-DA 10 μM, incubation time 30 min, $T = 37$ °C. Dendrimer concentrations 12.5–100 μM (fluorescence), 50 μM (confocal microscopy). The effects of dendrimers were compared with those of caffeic acid and other antioxidants such as melatonin or ascorbic acid at the same concentrations. Values are expressed as mean ± SD ($n = 3$).

continuously [48–53]. Functionalizing these systems, exploiting the multivalency of dendrimer skeletons using molecules with various therapeutic activities, has made it possible to reduce toxicity, increase bioavailability and improve activity. The properties of these nanoparticles can be improved for biomedical purposes. This improvement can take several directions, the first being to modify dendrimers with other active molecules such as metals [23,24,26,55,56] or polyethylene glycol [57–59] to improve their anticancer properties [23,24,56,60], reduce toxicity and increase bioavailability [24,59,61,62]. In another direction, the medical properties of dendrimers can be enhanced by conjugating them with natural biomolecules such as polyphenols [31,44,63].

Polyphenols are good natural antioxidants. Their physicochemical properties enable them to participate in various cellular redox-type metabolic reactions and prevent cells from being injured by ROS [44,64,65]. However, they are generally poorly absorbed by the intestines, rapidly metabolized, and quickly excreted. These factors limit their bioavailability [44,66].

To address these shortcomings, we have synthesized carbosilane dendritic systems containing one or two caffeic acid units, and ammonium groups on the surface to make them water soluble. The polyphenol is anchored to the dendritic skeleton by amidation, either on a dendritic branch functionalized with $HS(CH_2)_2NH_2$ (compounds **7–8**) or HS-PEG-NH_2 (MW = 3.5 kDa, compounds **9–10**). Cationic systems **15**–**18** were obtained by quaternization of the dimethylammonium groups on the remaining dendritic branches. Their structural characterization by one- and two-dimensional NMR and elemental analysis is consistent with their proposed structures. Considering their potential use as antioxidants, we have studied their antioxidant activity including their ability to protect living cells under oxidative stress conditions. We have also characterized their biophysical properties.

Their hydrodynamic diameter ranged from 200 to 500 nm depending on the dendrimer, but the sizes ranged widely from 10 to 1000 nm. This could indicate the tendency of dendrimers to form assembled structures. The size of other carbosilane dendrimers has been reported as 150 nm to 500 nm [7],. The PDI of the dendrimers, which indicates the uniformity and homogeneity of a nanoparticle distribution, was about 0.4, except for dendrimer **18,** which contains two caffeic acid moieties and PEG.

To confirm the results from DLS we examined the morphology of dendrimers **15**–**18** by TEM. They were visible as single dots less than 5–10 nm in diameter. Dendrimers are usually shown as aggregate structures on TEM images [68,69], probably because interaction between nanoparticles leading to larger structures. The discrepancy between DLS and TEM results has been described in more detail previously [4].

Another aim was to investigate the surface charge of the dendrimers studied. On the basis of zeta potential values, we inferred that all heterofunctionalized dendrimers were positively charged. However, dendrimers containing PEG had lower zeta potentials than PEG-free dendrimers, 3 mV (**17**–**18**) vs 20 mV (**15**–**16**). These results indicate that

PEG in a dendrimer scaffold decreases the net charge, with beneficial effects such as prolonged circulation time, lower cytotoxicity, reduced reactions with serum proteins, and stabilization of interactions with nucleic acids [6,20].

Toxicity profiles of potential therapeutic agents should be defined in vitro before their application in vivo. Therefore, the next step in this study was to evaluate dendrimer cytotoxicity. The cytotoxicity towards both cell lines tested (BJ and A549) was low. Similarly, other polyphenolic dendrimers showed no negative effect on PBM [70], HFF-1 [44] or CHO-K1 cells [71]. Dendrimers containing vanillin were cytotoxic against PC3 and HeLa cells [63]. It should be noted that the types of terminal end group in carbosilane dendrimers determined their toxicity towards different kinds of cells [60].

One of the most important findings of this study was that polyphenolic dendrimers have antioxidant activity. They were effective in scavenging free radicals, inhibiting AAPH-induced haemolysis and lipid peroxidation, and decreasing the ROS level. For the first time we investigated the ability of dendrimers to scavenge free radicals using the DPPH and FRAP assay. The addition of any of the dendrimers to an ethanol solution of the free radical was effective in free radical scavenging. Among the concentrations used, 100 μM had the most pronounced effect, having a scavenging effect of 7% or more. Similar results for other polyphenolic dendrimers had been demonstrated previously. For example, carbosilane dendrimers containing vanillin exhibited high antiradical potential [63]. The same effect was shown for dendritic polyphenol molecules [71] and polyphenol-based dendrimers [71]. Analysis of the antiradical activity in reaction with DPPH showed that PEG-free dendrimers showed weak change in antiradical activity. However, there was a visible difference for dendrimers containing PEG. A similar trend was observed in the FRAP assay. It has been shown that heterofunctionalized systems have lower activity than homofunctionalized ones [44]. Nevertheless, their activity is comparable to free caffeic acid, with the advantage of increasing the bioavailability of caffeic acid owing to the presence of ammonium groups on the surface, which confer high solubility in water.

The antioxidant properties of polyphenols have been presented many times [72,73]. Free radicals are produced during metabolic activity in cells, but if they reach high levels then cell structures can be damaged irreversibly [71].

We have also demonstrated that polyphenolic dendrimers with ammonium moieties on the surface inhibit AAPH-induced lipid peroxidation in erythrocyte membranes. The new dendritic systems could protect erythrocyte membranes against oxidative damage. AAPH increased the level of lipid peroxidation, but preincubation with dendrimers significantly inhibited this effect in a concentration-dependent manner; 50–100 μM concentrations showed most pronounced effect, almost equal to that of caffeic acid.

Since the newly synthesized systems had proved highly effective in free radical scavenging and inhibition of lipid peroxidation, we hypothesized that the dendrimers could protect human erythrocytes from induced oxidative stress. The anti-haemolytic effect of dendrimers on AAPH-induced oxidative haemolysis was investigated by preincubating erythrocytes with them. AAPH increases haemolysis by increasing intracellular free radical production [74,75]. The free radicals attack the erythrocyte membrane, altering the constituent lipids and proteins and inducing haemolysis.

Treating the erythrocytes with dendrimers before AAPH exposure drastically decreased the level of oxidative haemolysis. Other natural compounds such as catechins and polyphenols efficiently protect human erythrocytes against haemolysis induced by oxidative stress [76–78].

Evidence shows that increased haemolysis induced by oxidative stress is associated with activation of cellular ROS production [74]. Our results confirm this, showing an increased ROS level in human fibroblasts after treatment with AAPH. Treatment of BJ cells with polyphenolic dendrimers (50–100 μM) significantly decreased the intracellular level of ROS, protecting the cells against damage induced by oxidative stress. We previously reported a similar effect when BJ cells were treated with antioxidant plant extracts isolated from *Hippophae rhamnoides* L. and *Rosa canina* L. [79,80]. Both extracts were rich in natural antioxidants including polyphenols [79,80]. It has been documented that polyphenols decrease ROS levels in different kinds of cells such as dermal fibroblasts [81], PC12 [82], and kidney mesangial cells [83].

Summarizing, the dendrimers studied had low cytotoxicity and showed high antioxidant potential comparable with known antioxidants. Therefore, caffeic acid in their structure can quench free radicals, protecting the cells against oxidative stress.

5. Conclusions

This work has demonstrated that conjugation of polyphenols with cationic carbosilane dendrimers could be a promising way of harnessing the potential of these powerful antioxidants, significantly increasing their bioavailability. Therefore, a new water-soluble family of carbosilane dendrimers functionalized with caffeic acid and surface ammonium groups has been synthesized. The most important outcome is that these dendritic systems have low toxiciy and are highly effective against oxidative stress in vitro. Their antioxidant property could help to diminish oxidative haemolysis, lipid peroxidation, and ROS levels via their ability to scavenge free radicals. These findings are confirmed by various biological tests including in vitro studies on human fibroblasts, erythrocytes and A549 cells.

CRediT authorship contribution statement

Marika Grodzicka: Investigation, Data curation, Writing – original draft. **Cornelia E. Pena-Gonzalez:** Investigation, Data curation, Writing – original draft. **Paula Ortega:** Methodology, Validation, Supervision, Data curation, Writing – review & editing. **Sylwia Michlewska:** Visualization, Validation, Investigation, Writing – review & editing. **Rebeca Lozano:** Investigation, Software, Validation. **Maria Bryszewska:** Writing – review & editing. **Francisco Javier de la Mata:** Supervision, Conceptualization, Methodology, Writing – review & editing. **Maksim Ionov:** Conceptualization, Methodology, Supervision, Writing – review & editing.

Declaration of Competing Interest

The authors declare no conflict of interest.

Acknowledgements

This work was co-financed by the Project "EUROPARTNER" of Polish National Agency for Academic Exchange (NAWA) project No: PPI/APM/2018/1/00007/U/001 and partly granted by the Project "Np-Hale" under Beethoven Life 1 program of National Science Centre of Poland (NCN) project No: 2018/31/F/NZ5/03454. Grants from PID2020-112924RBI00 (MINECO), and project SBPLY/17/180501/000358 Junta de Comunidades de Castilla-La Mancha (JCCM), PID2019-104070RB-C22 (MICINN) consortiums IMMUNOTHERCAN-CM B2017/BMD-3733 and NANODENDMED II-CM ref. B2017/BMD-3703. CIBER-BBN is an initiative funded by the VI National R&D&i Plan 2008-2011, Iniciativa Ingenio 2010, the Consolider Program, and CIBER Actions and financed by the Instituto de Salud Carlos III with assistance from the European Regional Development Fund.

Appendix A. Supplementary data

Supplementary data to this article can be found online at https://doi.org/10.1016/j.susmat.2022.e00497.

References

[1] Z. Lyu, L. Ding, A.Y.T. Huang, C.L. Kao, L. Peng, Poly(amidoamine)dendrimers: covalent and supramolecular synthesis, Mater. Today Chem. 13 (2019) 34–48, https://doi.org/10.1016/j.mtchem.2019.04.004.

[2] D.A. Tomalia, H. Baker, J. Dewald, M. Hall, G. Kallos, S. Martin, J. Roeck, J. Ryder, P. Smith, A new class of polymers: starburst-dendritic macromolecules, Polym. J. 17 (1985) 117–132, https://doi.org/10.1295/polymj.17.117.

[3] P. Pandi, A. Jain, N. Kommineni, M. Ionov, M. Bryszewska, W. Khan, Dendrimer as a new potential carrier for topical delivery of siRNA: A comparative study of dendriplex vs. lipoplex for delivery of TNF-α siRNA, Int. J. Pharm. 550 (2018) 240–250, https://doi.org/10.1016/j.ijpharm.2018.08.024.

[4] M. Ionov, K. Ciepluch, B. Klajnert, S. Glińska, R. Gomez-Ramirez, F.J. de la Mata, M.A. Munoz-Fernandez, M. Bryszewska, Complexation of HIV derived peptides with carbosilane dendrimers, Colloids Surf. B: Biointerfaces 101 (2013) 236–242, https://doi.org/10.1016/j.colsurfb.2012.07.011.

[5] P. Kesharwani, L. Xie, G. Mao, S. Padhye, A.K. Iyer, Hyaluronic acid-conjugated polyamidoamine dendrimers for targeted delivery of 3,4-difluorobenzylidene curcumin to CD44 overexpressing pancreatic cancer cells, Colloids Surf. B: Biointerfaces 136 (2015) 413–423, https://doi.org/10.1016/j.colsurfb.2015.09.043.

[6] S. Thakur, P. Kesharwani, R.K. Tekade, N.K. Jain, Impact of pegylation on biopharmaceutical properties of dendrimers, Polymer (Guildf). 59 (2015) 67–92, https://doi.org/10.1016/j.polymer.2014.12.051.

[7] S. Michlewska, M. Ionov, D. Shcharbin, M. Maroto-Díaz, R. Gomez Ramirez, F. Javier de la Mata, M. Bryszewska, Ruthenium metallodendrimers with anticancer potential in an acute promyelocytic leukemia cell line (HL60), Eur. Polym. J. 87 (2017) 39–47, https://doi.org/10.1016/j.eurpolymj.2016.12.011.

[8] S. Michlewska, M. Ionov, M. Maroto-Díaz, A. Szwed, A. Ihnatsyeu-Kachan, S. Loznikova, D. Shcharbin, M. Maly, R.G. Ramirez, F.J. de la Mata, M. Bryszewska, Ruthenium dendrimers as carriers for anticancer siRNA, J. Inorg. Biochem. 181 (2018), https://doi.org/10.1016/j.jinorgbio.2018.01.001.

[9] N.S. Del Olmo, M. Holota, S. Michlewska, R. Gómez, P. Ortega, M. Ionov, F.J. de la Mata, M. Bryszewska, Copper (II) metallodendrimers combined with pro-apoptotic sirnas as a promising strategy against breast cancer cells, Pharmaceutics. 12 (2020) 1–14, https://doi.org/10.3390/pharmaceutics12080727.

[10] E. Pedziwiatr-Werbicka, K. Milowska, V. Dzmitruk, M. Ionov, D. Shcharbin, M. Bryszewska, Dendrimers and hyperbranched structures for biomedical applications, Eur. Polym. J. 119 (2019) 61–73, https://doi.org/10.1016/j.eurpolymj.2019.07.013.

[11] O. Sytar, I. Hemmerich, M. Zivcak, C. Rauh, M. Brestic, Comparative analysis of bioactive phenolic compounds composition from 26 medicinal plants, Saudi, J. Biol. Sci. 25 (2018) 631–641, https://doi.org/10.1016/j.sjbs.2016.01.036.

[12] O.A. Krasheninina, E.K. Apartsin, E. Fuentes, A. Szulc, M. Ionov, A. G. Venyaminova, D. Shcharbin, F.J. de la Mata, M. Bryszewska, R. Gómez, R. Gómez, Complexes of pro-apoptotic sirnas and carbosilane dendrimers: formation and effect on cancer cells, Pharmaceutics. 11 (2019) 25, https://doi.org/10.3390/pharmaceutics11010025.

[13] A. Jain, S. Mahira, J.-P. Majoral, M. Bryszewska, W. Khan, M. Ionov, Dendrimer mediated targeting of siRNA against polo-like kinase for the treatment of triple negative breast cancer, J. Biomed. Mater. Res. Part A. 107 (2019) 1933–1944, https://doi.org/10.1002/jbm.a.36701.

[14] K. Białkowska, K. Miłowska, S. Michlewska, P. Sokołowska, P. Komorowski, T. Lozano-Cruz, R. Gomez-Ramirez, F.J. de la Mata, M. Bryszewska, Interaction of cationic carbosilane dendrimers and their siRNA complexes with MCF-7 cells, Int. J. Mol. Sci. 22 (2021), https://doi.org/10.3390/ijms22137097.

[15] M. Ionov, Z. Garaiova, I. Waczulikova, D. Wróbel, E. Pędziwiatr-Werbicka, R. Gomez-Ramirez, F.J. De La Mata, B. Klajnert, T. Hianik, M. Bryszewska, siRNA carriers based on carbosilane dendrimers affect zeta potential and size of phospholipid vesicles, Biochim. Biophys. Acta Biomembr. 2012 (1818) 2209–2216, https://doi.org/10.1016/j.bbamem.2012.04.019.

[16] J. Lazniewska, K. Milowska, N. Katir, A. El Kadib, M. Bryszewska, J.P. Majoral, T. Gabryelak, Viologen-phosphorus dendrimers exhibit minor toxicity against a murine neuroblastoma cell line, Cell. Mol. Biol. Lett. 18 (2013) 459–478, https://doi.org/10.2478/s11658-013-0100-5.

[17] K. Jain, P. Kesharwani, U. Gupta, N.K. Jain, Dendrimer toxicity: Let's meet the challenge, Int. J. Pharm. 394 (2010) 122–142, https://doi.org/10.1016/j.ijpharm.2010.04.027.

[18] S. Svenson, Dendrimers as versatile platform in drug delivery applications, Eur. J. Pharm. Biopharm. 71 (2009) 445–462, https://doi.org/10.1016/j.ejpb.2008.09.023.

[19] V. Patel, C. Rajani, D. Paul, P. Borisa, K. Rajpoot, S.R. Youngren-Ortiz, R.K. Tekade, Dendrimers as Novel Drug-Delivery System and its Applications, Elsevier Inc., 2019, https://doi.org/10.1016/B978-0-12-814487-9.00008-9.

[20] S. Somani, P. Laskar, N. Altwaijry, P. Kewcharoenvong, C. Irving, G. Robb, B. S. Pickard, C. Dufès, PEGylation of polypropylenimine dendrimers: effects on cytotoxicity, DNA condensation, gene delivery and expression in cancer cells, Sci. Rep. 8 (2018) 1–13, https://doi.org/10.1038/s41598-018-27400-6.

[21] Y. Jin, X. Ren, W. Wang, L. Ke, E. Ning, L. Du, J. Bradshaw, A 5-fluorouracil-loaded pH-responsive dendrimer nanocarrier for tumor targeting, Int. J. Pharm. 420 (2011) 378–384, https://doi.org/10.1016/j.ijpharm.2011.08.053.

[22] S. Spreckelmeyer, C. Orvig, A. Casini, Cellular transport mechanisms of cytotoxic metallodrugs: an overview beyond cisplatin, Molecules. 19 (2014) 15584–15610, https://doi.org/10.3390/molecules191015584.

[23] S. Michlewska, M. Ionov, A. Szwed, A. Rogalska, N.S. Del Olmo, P. Ortega, M. Denel, D. Jacenik, D. Shcharbin, F.J. de la Mata, M. Bryszewska, Ruthenium dendrimers against human lymphoblastic leukemia 1301 cells, Int. J. Mol. Sci. 21 (2020) 1–13, https://doi.org/10.3390/ijms21114119.

[24] S. Michlewska, M. Maroto, M. Hołota, M. Kubczak, N. Sanz del Olmo, P. Ortega, D. Shcharbin, F.J. de la Mata, M. Bryszewska, M. Ionov, Combined therapy of ruthenium dendrimers and anti-cancer drugs against human leukemic cells, Dalton Trans. (2021) 9500–9511, https://doi.org/10.1039/d1dt01388b.

[25] M. Hołota, J. Magiera, S. Michlewska, M. Kubczak, N.S.D.N.S. Del Olmo, S. García-Gallego, P. Ortega, F.J.J. De La Mata, M. Ionov, M. Bryszewska, In vitro anticancer properties of copper metallodendrimers, Biomolecules. 9 (2019) 1–15, https://doi.org/10.3390/biom9040155.

[26] N. Sanz del Olmo, M. Maroto-Díaz, R. Gómez, P. Ortega, M. Cangiotti, M. F. Ottaviani, F.J. de la Mata, Carbosilane metallodendrimers based on copper (II) complexes: synthesis, EPR characterization and anticancer activity, J. Inorg. Biochem. 177 (2017) 211–218, https://doi.org/10.1016/j.jinorgbio.2017.09.023.

[27] S. Alfei, B. Marengo, C. Domenicotti, Polyester-based dendrimer nanoparticles combined with etoposide have an improved cytotoxic and pro-oxidant effect on human neuroblastoma cells, Antioxidants. 9 (2020) 1–23, https://doi.org/10.3390/antiox9010050.

[28] S. Ku, F. Yan, Y. Wang, Y. Sun, N. Yang, L. Ye, The blood-brain barrier penetration and distribution of PEGylated fluorescein-doped magnetic silica nanoparticles in rat brain, Biochem. Biophys. Res. Commun. 394 (2010) 871–876, https://doi.org/10.1016/j.bbrc.2010.03.006.

[29] E. Lopez-Lopez, W.E. Evans, New insights into methotrexate accumulation in leukemia cells in vivo, Mol. Cell. Oncol. 8 (2021) 1865086, https://doi.org/10.1080/23723556.2020.1865086.

[30] M. Valko, D. Leibfritz, J. Moncol, M.T.D. Cronin, M. Mazur, J. Telser, Free radicals and antioxidants in normal physiological functions and human disease, Int. J. Biochem. Cell Biol. 39 (2007) 44–84, https://doi.org/10.1016/j.biocel.2006.07.001.

[31] S. Alfei, B. Marengo, G. Zuccari, F. Turrini, C. Domenicotti, Dendrimer nanodevices and gallic acid as novel strategies to fight chemoresistance in neuroblastoma cells, Nanomaterials. 10 (2020) 1–30, https://doi.org/10.3390/nano10061243.

[32] C.-L. Ky, J. Louarn, S. Dussert, B. Guyot, S. Hamon, M. Noirot, Caffeine, trigonelline, chlorogenic acids and sucrose diversity in wild *Coffea arabica* L. and *C. canephora* P. accessions, Food Chem. 75 (2001) 223–230, https://doi.org/10.1016/S0308-8146(01)00204-7.

[33] J.A. Greenberg, C.N. Boozer, A. Geliebter, Coffee, diabetes, and weight control, Am. J. Clin. Nutr. 84 (2006) 682–693, https://doi.org/10.1093/ajcn/84.4.682.

[34] E. Choi, K.-H. Choi, S.M. Park, D. Shin, H.-K. Joh, E. Cho, The benefit of bone health by drinking coffee among Korean postmenopausal women: A cross-sectional analysis of the fourth & fifth Korea National Health and nutrition examination surveys, PLoS One 11 (2016), e0147762, https://doi.org/10.1371/journal.pone.0147762.

[35] B. Shukitt-Hale, M.G. Miller, Y.F. Chu, B.J. Lyle, J.A. Joseph, Coffee, but not caffeine, has positive effects on cognition and psychomotor behavior in aging, Age (Omaha). 35 (2013) 2183–2192, https://doi.org/10.1007/s11357-012-9509-4.

[36] S. Ni, Y. Xie, Y. Tang, Y. Liu, J. Chen, S. Zhu, N-2-hydroxypropyltimehyl ammonium chloride chitosan nanoparticles for siRNA pulmonary delivery: preparation, characterization and in vitro evaluation, J. Drug Target. 25 (2017) 451–462, https://doi.org/10.1080/1061186X.2016.1278219.

[37] Pevzner, 乳鼠心肌提取 HHS public access, Physiol. Behav. 176 (2017) 139–148, https://doi.org/10.1158/1055-9965.EPI-15-0924.Coffee.

[38] Y.-M. Li, J. Peng, L.-Z. Li, Coffee consumption associated with reduced risk of Oral cancer: a meta-analysis, Oral Surg, Oral Med. Oral Pathol. Oral Radiol. 121 (2016) 381–389.e1, https://doi.org/10.1016/j.oooo.2015.12.006.

[39] E. Loftfield, N.D. Freedman, B.I. Graubard, A.R. Hollenbeck, F.M. Shebl, S. T. Mayne, R. Sinha, Coffee drinking and cutaneous melanoma risk in the NIH-AARP diet and health study, J. Natl. Cancer Inst. 107 (2015) 1–9, https://doi.org/10.1093/jnci/dju421.

[40] M. Lukic, M. Jareid, E. Weiderpass, T. Braaten, Coffee consumption and the risk of malignant melanoma in the Norwegian women and Cancer (NOWAC) study, BMC Cancer 16 (2016), https://doi.org/10.1186/s12885-016-2586-5.

[41] M. Koga, S. Nakagawa, A. Kato, I. Kusumi, Caffeic acid reduces oxidative stress and microglial activation in the mouse hippocampus, Tissue Cell 60 (2019) 14–20, https://doi.org/10.1016/j.tice.2019.07.006.

[42] K.M. Monteiro Espíndola, R.G. Ferreira, L.E. Mosquera Narvaez, A.C. Rocha Silva Rosario, A.H. Machado Da Silva, A.G. Bispo Silva, A.P. Oliveira Vieira, M. Chagas Monteiro, Chemical and pharmacological aspects of caffeic acid and its activity in hepatocarcinoma, Front. Oncol. 9 (2019) 3–5, https://doi.org/10.3389/fonc.2019.00541.

[43] D. Guo, D. Dou, L. Ge, Z. Huang, L. Wang, N. Gu, A caffeic acid mediated facile synthesis of silver nanoparticles with powerful anti-cancer activity, Colloids Surf. B: Biointerfaces 134 (2015) 229–234, https://doi.org/10.1016/j.colsurfb.2015.06.070.

[44] N.S. Del Olmo, C.E.P. González, J.D. Rojas, R. Gómez, P. Ortega, A. Escarpa, F.J. de la Mata, Antioxidant and antibacterial properties of carbosilane dendrimers functionalized with polyphenolic moieties, Pharmaceutics. 12 (2020) 1–16, https://doi.org/10.3390/pharmaceutics12080698.

[45] E.M. Egorova, The validity of the Smoluchowski equation in electrophoretic studies of lipid membranes, Electrophoresis. 15 (1994) 1125–1131, https://doi.org/10.1002/elps.11501501170.

[46] M. Galán, E. Fuentes-Paniagua, F.J. de la Mata, R. Gómez, Heterofunctionalized Carbosilane dendritic systems: Bifunctionalized Dendrons as building blocks versus statistically decorated dendrimers, Organometallics. 33 (2014) 3977–3989, https://doi.org/10.1021/om500464k.

[47] E. Fuentes-Paniagua, M.J. Serramía, J. Sánchez-Nieves, S. Álvarez, M.Á. Muñoz-Fernández, R. Gómez, F.J. De La Mata, Fluorescein labelled cationic carbosilane dendritic systems for biological studies, Eur. Polym. J. 71 (2015) 61–72, https://doi.org/10.1016/j.eurpolymj.2015.07.043.

[48] X. Yan, Y. Yang, Y. Sun, Dendrimer applications for Cancer therapies, J. Phys. Conf. Ser. 1948 (2021), https://doi.org/10.1088/1742-6596/1948/1/012205.

[49] B. Noriega-Luna, L.A. Godínez, F.J. Rodríguez, A. Rodríguez, G. Zaldívar-Lelo De Larrea, C.F. Sosa-Ferreyra, R.F. Mercado-Curiel, J. Manríquez, E. Bustos, Applications of dendrimers in drug delivery agents, diagnosis, therapy, and detection, J. Nanomater. 2014 (2014), https://doi.org/10.1155/2014/507273.

[50] A.P. Sherje, M. Jadhav, B.R. Dravyakar, D. Kadam, Dendrimers: A versatile nanocarrier for drug delivery and targeting, Int. J. Pharm. 548 (2018) 707–720, https://doi.org/10.1016/j.ijpharm.2018.07.030.

[51] S. Svenson, D.A. Tomalia, Dendrimers in biomedical applications - reflections on the field, Adv. Drug Deliv. Rev. 57 (2005) 2106–2129, https://doi.org/10.1016/j.addr.2005.09.018.

[52] P. Kesharwani, S. Banerjee, U. Gupta, M.C.I. Mohd Amin, S. Padhye, F.H. Sarkar, A. K. Iyer, PAMAM dendrimers as promising nanocarriers for RNAi therapeutics, Mater. Today 18 (2015) 565–572, https://doi.org/10.1016/j.mattod.2015.06.003.

[53] N. Martinho, H. Florindo, L. Silva, S. Brocchini, M. Zloh, T. Barata, Molecular modeling to study dendrimers for biomedical applications, Molecules. 19 (2014) 20424–20467, https://doi.org/10.3390/molecules191220424.

[55] M. Maroto-Díaz, B.T. Elie, P. Gómez-Sal, J. Pérez-Serrano, R. Gómez, M. Contel, F. Javier De La Mata, Synthesis and anticancer activity of carbosilane metallodendrimers based on arene ruthenium(ii) complexes, Dalton Trans. 45 (2016) 7049–7066, https://doi.org/10.1039/c6dt00465b.

[56] M. Maroto-Diaz, N. Sanz del Olmo, L. Muñoz-Moreno, A.M. Bajo, M.J. Carmena, R. Gómez, S. García-Gallego, F.J. de la Mata, In vitro and in vivo evaluation of first-generation carbosilane arene Ru(II)-metallodendrimers in advanced prostate cancer, Eur. Polym. J. 113 (2019) 229–235, https://doi.org/10.1016/j.eurpolymj.2019.01.047.

[57] A.M. Master, M.E. Rodriguez, M.E. Kenney, N.L. Oleinick, A. Sen Gupta, Delivery of the photosensitizer Pc 4 in PEG–PCL micelles for in vitro PDT studies, J. Pharm. Sci. 99 (2010) 2386–2398, https://doi.org/10.1002/jps.

[58] T. Sadat, J. Kashi, S. Eskandarion, M. Esfandyari-Manesh, S. Mahmoud, A. Marashi, N. Samadi, S.M. Fatemi, F. Atyabi, S. Eshraghi, R. Dinarvand, Improved drug loading and antibacterial activity of minocycline-loaded PLGA nanoparticles prepared by solid/oil/water ion pairing method, Int. J. Nanomedicine 2 (2012) 221–234, https://doi.org/10.2147/ijn.s27709.

[59] A. Janaszewska, J. Lazniewska, P. Trzepiński, M. Marcinkowska, B. Klajnert-Maculewicz, Cytotoxicity of dendrimers, Biomolecules. 9 (2019) 1–23, https://doi.org/10.3390/biom9080330.

[60] S. Michlewska, M. Ionov, M. Maroto-Díaz, A. Szwed, A. Ihnatsyeu-Kachan, V. Abashkin, V. Dzmitruk, A. Rogalska, M. Denel, M. Gapinska, D. Shcharbin, R. Gomez Ramirez, F.J. De La Mata, M. Bryszewska, Ruthenium dendrimers against acute promyelocytic leukemia: in vitro studies on HL-60 cells, Future Med. Chem. 11 (2019), https://doi.org/10.4155/fmc-2018-0274.

[61] Y. Chang, N. Liu, L. Chen, X. Meng, Y. Liu, Y. Li, J. Wang, Synthesis and characterization of DOX-conjugated dendrimer-modified magnetic iron oxide conjugates for magnetic resonance imaging, targeting, and drug delivery, J. Mater. Chem. 22 (2012) 9594–9601, https://doi.org/10.1039/c2jm16792a.

[62] D. Luong, P. Kesharwani, R. Deshmukh, M.C.I. Mohd Amin, U. Gupta, K. Greish, A. K. Iyer, PEGylated PAMAM dendrimers: enhancing efficacy and mitigating toxicity for effective anticancer drug and gene delivery, Acta Biomater. 43 (2016) 14–29, https://doi.org/10.1016/j.actbio.2016.07.015.

[63] G. Mencia, N.S. Del Olmo, L. Muñoz-Moreno, M. Maroto-Diaz, R. Gomez, P. Ortega, M. José Carmena, F. Javier de la Mata, Polyphenolic carbosilane dendrimers as anticancer agents against prostate cancer, New J. Chem. 40 (2016) 10488–10497, https://doi.org/10.1039/c6nj02545e.

[64] F. Visioli, G. Bellomo, C. Galli, Free radical-scavenging properties of olive oil polyphenols, Biochem. Biophys. Res. Commun. 247 (1998) 60–64, https://doi.org/10.1006/bbrc.1998.8735.

[65] Y. Hanasaki, S. Ogawa, S. Fukui, The correlation between active oxygens scavenging and antioxidative effects of flavonoids, Free Radic. Biol. Med. 16 (1994) 845–850, https://doi.org/10.1016/0891-5849(94)90202-X.

[66] D.D. Milinčić, D.A. Popović, S.M. Lević, A. Kostić, Ž.L. Tešić, V.A. Nedović, M. B. Pešić, Application of polyphenol-loaded nanoparticles in food industry, Nanomaterials. 9 (2019), https://doi.org/10.3390/nano9111629.

[68] N. Katir, N. Marcotte, S. Michlewska, M. Ionov, N. El Brahmi, M. Bousmina, J. P. Majoral, M. Bryszewska, A. El Kadib, Dendrimer for templating the growth of porous catechol-coordinated titanium dioxide frameworks: toward Hemocompatible nanomaterials, ACS Appl. Nano Mater. 2 (2019), https://doi.org/10.1021/acsanm.9b00382.

[69] S. Michlewska, M. Kubczak, M. Maroto-Díaz, N.S. Del Olmo, P. Ortega, D. Shcharbin, R.G. Ramirez, F.J. De La Mata, M. Ionov, M. Bryszewska, Synthesis and characterization of FITC labelled ruthenium dendrimer as a prospective anticancer drug, Biomolecules. 9 (2019), https://doi.org/10.3390/biom9090411.

[70] E. Pedziwiatr-Werbicka, E. Fuentes, V. Dzmitruk, J. Sánchez-Nieves, M. Sudas, E. Drozd, A. Shakhbazau, D. Shcharbin, F.J. de la Mata, R. Gomez-Ramirez, M. A. Munoz-Fernandez, M. Bryszewska, Novel "SiC" carbosilane dendrimers as carriers for anti-HIV nucleic acids: studies on complexation and interaction with blood cells, Colloids Surf. B: Biointerfaces 109 (2013) 183–189, https://doi.org/10.1016/j.colsurfb.2013.03.045.

[71] W.H. Lee, C.Y. Loo, D. Traini, P.M. Young, Inhalation of nanoparticle-based drug for lung cancer treatment: advantages and challenges, Asian, J. Pharm. Sci. 10 (2015) 481–489, https://doi.org/10.1016/j.ajps.2015.08.009.

[72] M.E.E.-D. Ibrahim, R.M. Alqurashi, Anti-fungal and antioxidant properties of propolis (bee glue) extracts, Int. J. Food Microbiol. 361 (2022), 109463, https://doi.org/10.1016/j.ijfoodmicro.2021.109463.

[73] S.E. Owumi, C.E. Irozuru, U.O. Arunsi, A.K. Oyelere, Caffeic acid protects against DNA damage, oxidative and inflammatory mediated toxicities, and upregulated caspases activation in the hepatorenal system of rats treated with aflatoxin B1, Toxicon. 207 (2022) 1–12, https://doi.org/10.1016/j.toxicon.2021.12.021.

[74] H.-L. Yang, M. Korivi, M.-K. Lin, H.C.-W. Chang, C.-R. Wu, M.-S. Lee, W.T.-L. Chen, Y.-C. Hseu, Antihemolytic and antioxidant properties of pearl powder against 2,2′-azobis(2-amidinopropane) dihydrochloride-induced hemolysis and oxidative damage to erythrocyte membrane lipids and proteins, J. Food Drug Anal. 25 (2017) 898–907, https://doi.org/10.1016/j.jfda.2016.10.007.

[75] V.M. Barodka, E. Nagababu, J.G. Mohanty, D. Nyhan, D.E. Berkowitz, J.M. Rifkind, J.J. Strouse, New insights provided by a comparison of impaired deformability with erythrocyte oxidative stress for sickle cell disease, blood cells, Mol. Dis. 52 (2014) 230–235, https://doi.org/10.1016/j.bcmd.2013.10.004.

[76] T. Baccarin, M. Mitjans, E. Lemos-Senna, M.P. Vinardell, Protection against oxidative damage in human erythrocytes and preliminary photosafety assessment of Punica granatum seed oil nanoemulsions entrapping polyphenol-rich ethyl acetate fraction, Toxicol. in Vitro 30 (2015) 421–428, https://doi.org/10.1016/j.tiv.2015.09.020.

[77] C. Widén, A. Ekholm, M.D. Coleman, S. Renvert, K. Rumpunen, Erythrocyte antioxidant protection of rose hips (*Rosa* spp.), Oxidative Med. Cell. Longev. 2012 (2012), 621579, https://doi.org/10.1155/2012/621579.

[78] K. Naparlo, G. Bartosz, I. Stefaniuk, B. Cieniek, M. Soszynski, I. Sadowska-Bartosz, Interaction of catechins with human erythrocytes, Molecules. 25 (2020) 1–16, https://doi.org/10.3390/molecules25061456.

[79] M. Kubczak, A.B. Khassenova, B. Skalski, S. Michlewska, *Hippophae rhamnoides* L. leaf and twig extracts as rich sources of nutrients and bioactive compounds with antioxidant activity, Sci. Rep. (2022) 1–14, https://doi.org/10.1038/s41598-022-05104-2.

[80] M. Kubczak, A.B. Khassenova, B. Skalski, S. Michlewska, M. Wielanek, A. N. Aralbayeva, M.K. Murzakhmetova, M. Zamaraeva, M. Skłodowska, M. Bryszewska, M. Ionov, Bioactive compounds and antiradical activity of the Rosa canina L. leaf and twig extracts, Agronomy 10 (2020) 1–10.

[81] A. Darawsha, A. Trachtenberg, J. Levy, Y. Sharoni, The protective effect of carotenoids, polyphenols, and estradiol on dermal fibroblasts under oxidative stress, Antioxidants 10 (2021), https://doi.org/10.3390/antiox10122023.

[82] J.A.G. Crispo, D.R. Ansell, M. Piche, J.K. Eibl, N. Khaper, G.M. Ross, T.C. Tai, Protective effects of polyphenolic compounds on oxidative stress-induced cytotoxicity in PC12 cells, Can. J. Physiol. Pharmacol. 88 (2010) 429–438, https://doi.org/10.1139/Y09-137.

[83] H. Wang, D. Li, Z. Hu, S. Zhao, Z. Zheng, W. Li, Protective effects of green tea polyphenol against renal injury through ROS-mediated JNK-MAPK pathway in Lead exposed rats, Mol. Cell 39 (2016) 508–513, https://doi.org/10.14348/molcells.2016.2170.